Master's thesis

NTNU
Norwegian University of Science and Technology
Faculty of Natural Sciences
Department of Biology

Nellie Henriette Nilsen

Spatial genetic structure in Northern European Sphagnum squarrosum Crome in relation to its Arctic morph

Master's thesis in Biology – Biodiversity and Systematics
Supervisor: Kristian Hassel
Co-supervisor: Hans K. Stenøien, Lena Meleshko, Kjell Ivar Flatberg, and Magni O. Kyrkjeeide

September 2021

Arctic morph of Sphagnum squarrosum. Photo by Kjell Ivar Flatberg

NTNU
Norwegian University of Science and Technology

Nellie Henriette Nilsen

Spatial genetic structure in Northern European Sphagnum squarrosum Crome in relation to its Arctic morph

Master's thesis in Biology – Biodiversity and Systematics
Supervisor: Kristian Hassel
Co-supervisor: Hans K. Stenøien, Lena Meleshko, Kjell Ivar Flatberg, and Magni O. Kyrkjeeide
September 2021

Norwegian University of Science and Technology
Faculty of Natural Sciences
Department of Biology

NTNU
Norwegian University of Science and Technology

Abstract

The Arctic morph of *Sphagnum squarrosum* differs from the typical Boreal morph and has morphological similarities with *Sphagnum teres* which is closely related and may resemble *S. squarrosum* when growing in certain conditions. While previous studies have detected no genetic structure in *Sphagnum squarrosum*, the Arctic morph has never been explored in the context of species delimitation. I aimed to clarify the taxonomic status of the Arctic morph of *S. squarrosum* and its phylogenetic relationship with *S. teres* and *S. tundrae* with which it co-occurs at Svalbard. RADseq analysis was applied to 61 samples of the three study species from Svalbard, Norway, Finland, Estonia, Faroe Islands, Greenland, and Russia. The dataset was then analysed with STRUCTURE, RAxML, PCA, and F_{ST} was calculated. I found that the Arctic morph belongs within *S. squarrosum*, but I also found more spatial structure in the *S. squarrosum* than discovered in previous studies. The specimens of *S. squarrosum* from Svalbard, Arctic Greenland, and Arctic Norway are genetically more similar to each other than to samples south of the Arctic circle. Samples south of the Arctic circle formed two groups, one containing samples from Faroe Islands and South Norway, while the other encompassed samples from all the remaining locations. The genetic group containing the samples from Southern Norway and Faroe Islands was the most genetically dissimilar among the *S. squarrosum* samples and could be under emerging speciation.

Sammendrag

Den arktiske morfen til *Sphagnum squarrosum* skiller seg fra den typiske Boreale morfen og har morfologiske likheter med *S. teres* som er nært beslektet og kan ligne på *S. squarrosum* når den vokser under spesifikke forhold. Tidligere studier har ikke funnet genetisk struktur i *S. squarrosum* og den arktiske morfen har aldri vært undersøkt i sammenheng med artsavgrensning. Jeg hadde som mål å oppklare den taksonomiske statusen til den arktiske morfen av *S. squarrosum* og dens fylogenetiske forhold til *S. teres* og *S. tundrae* som vokser sammen med den på Svalbard. Det ble utført RADseq analyse av 61 prøver av de tre studieartene fra Svalbard, Norge, Finland, Estland, Færøyene, Grønland, og Russland. Datasettet ble analysert med STRUCTURE, RAxML, PCA og F_{ST} verdiene ble estimert. Jeg fastslo at den arktiske morfen tilhører *S. squarrosum*, men jeg fant mer geografisk struktur i *S. squarrosum* enn tidligere studier har oppdaget. Individene av *S. squarrosum* fra Svalbard, og de arktiske områdene av Grønland og Norge er genetisk mer lik hverandre enn prøver sør for den arktiske sirkelen. Prøver sør for den arktiske sirkelen dannet to grupper, den ene inneholdt individer fra Færøyene og Sør-Norge, mens den andre inneholdt individene fra alle de gjenværende lokalitetene. Den genetiske gruppen bestående av prøvene fra Færøyene og Sør-Norge var mest genetisk distinkt blant prøvene av *S. squarrosum* og kan være i ferd med å bli en egen art.

Acknowledgements

Great gratitude is extended to The Royal Norwegian Society of Sciences and Letters for financing this study through the I.K. Lykkes fund. I would also like to extend my gratitude to BBC Earth YouTube for financing an extra expedition on Svalbard. I thank the Governor of Svalbard for providing us with the permissions needed to sample *Sphagnum* in Svalbard.

The sequencing service was provided by the Norwegian Sequencing Centre (www.sequencing.uio.no), a national technology platform hosted by the University of Oslo and supported by the "Functional Genomics" and "Infrastructure" programs of the Research Council of Norway and the Southeastern Regional Health Authorities.

I want to extend a deep thank you to Sarah L. Fordyce Martin for doing the library prep for me in the lab, I wish I could have been there, but Covid-19 restrictions were in place. A special thanks to Ronja Marie Hundal for the many hours of digital study sessions, without them the writing of this thesis would have been a lonely endeavour.

Last but absolutely not least I want to extend my deepest gratitude to my advisors who tirelessly helped me increase the quality of my work from start to finish.

Contents

Introduction

Biodiversity is of great importance to human society (Gamfeldt et al., 2008), nevertheless the result of human activities greatly reduce biodiversity (López-Rojo et al., 2019) at a speed that is not being matched by taxonomic research (Coleman, 2015). Species, genetic, and ecosystem diversity make up the foundation of biodiversity (Dewoody et al., 2021) which raises the level of ecosystem function providing goods and services to human society (Gamfeldt et al., 2008). Conserving genetic diversity within a species is not given the same attention as conserving species (Hedenäs, 2019) although it offers great predictive value on fitness, and adaptability of a species which could greatly aid in directing conservation efforts (Dewoody et al., 2021). Human impact such as climate change, pollution, and habitat loss decreases genetic diversity, biodiversity and subsequently ecosystem function multifunctionality in plants (López-Rojo et al., 2019). The extinction rates are inferred to be tens to hundreds of times higher than the natural background extinction rates and are accelerating (IPBES, 2019). Estimates of the number of species on earth vary from 1.8 to 14 million but either case leaves 21-86% of terrestrial species and 24-91% of marine species undescribed (Coleman, 2015). Despite this, the number of species experts is declining and many institutions and museums have policies that indirectly but noticeably impede taxonomic work (Coleman, 2015). The importance of biodiversity and loss thereof makes it an urgent field to study and makes it increasingly important to discover population subdivision as well as new species to guide the conservation efforts (López-Rojo et al., 2019).

Speciation occurs in a plethora of ways, and the dispersal mode of bryophytes could impact their demographic histories relative to seed plants. The diversity of sexually reproducing organisms we are surrounded by today stems from different modes of speciation, i.e., allopatric, sympatric, peripatric, polyploid, and hybrid speciation. Some of these processes have been shown in bryophytes (Meleshko et al., 2018; Shaw & Goffinet, 2008), spore producing non-vascular plants. Bryophytes have a strong dispersal potential of spores which could prevent isolation of populations by distance like seen in seed plants (Szövényi et al., 2012). For instance, the level of endemism in bryophytes is significantly lower than that displayed by angiosperms (Vanderpoorten et al., 2011).

Sphagnum or peat mosses is a genus in *Sphagnaceae*, one of the oldest bryophyte families, holding a tremendous amount of phenotypic variation (Flatberg, 1988, 2013; Stenøien et al., 2014) and is of great importance for the global carbon cycle (Yu et al., 2011). *Sphagnum* species are key components in the formation of peatlands (Flatberg, 2013) most of

which are located in the Northern Hemisphere above 45°N (Yu et al., 2011). Peatmosses cover only 3% of the world's land area, but store 25-30% of the world's soil stored carbon (Yu et al., 2010) which makes conservation of peatlands is vital in combating climate change.

Sphagnum squarrosum Crome subgenus *Acutifolia* described in 1803, has its distribution across the Northern Hemisphere with some occurrences in the Southern Hemisphere (GBIF_Secretariat, 2021). Historically, the large morphological diversity of *S. squarrosum* has been categorized by scientists into new species, subspecies, or varieties although none of these classifications persisted (Tropicos, 2021). The abundance of morphological characters stem in part from phenotypic plasticity found within *Sphagnum* and its ability to morphologically adapt to microclimates within its niche (Flatberg, 1988, 2013; Stenøien et al., 2014). As a result, many closely related species are hard to tell apart (Kyrkjeeide et al., 2015), which is the case for *S. squarrosum* and another species from subgenus *Acutifolia*, *S. teres* (Schimp.) Ångstr. ex Hartm.. When the two are growing under optimal conditions, the squarrose branch leaves that make *S. squarrosum* easy to recognize (Suzuki, 1967) help separate it from *S. teres*, along with several other characters (Flatberg, 2013). However, differentiating between the two species becomes increasingly difficult when different forms of *S. squarrosum* or *S. teres* exhibit morphology intermediate between the species (Society, 2010). Unfavourable environmental conditions are hypothesized to be the underlying cause of some of the morphs of *S. squarrosum* that resemble *S. teres* the most (Andrews, 1913). Depending on the habitat, *S. squarrosum* can vary in colouration: in the shade of forests they appear green with a light stem; but when exposed to sunlight they gain a slight yellow-brown colouration and a brown-ish stem, thereby resembling *S. teres* (Flatberg, 2013). The *S. squarrosum* forms that are the most difficult to differentiate from *S. teres* have been reported in North America (Andrews, 1913) and Japan (Suzuki, 1967). In turn, individuals of *S. teres* growing in the shade have greener shoots with branch leaves that curve away from the branch more than usual, thus resembling small individuals of *S. squarrosum* (Andrews, 1913; Flatberg, 2013; Society, 2010).

Like other plants (Peterson, 2014), many *Sphagnum* species such as *S. warnstorfii* Russow, *S. teres*, *S. obtusum* Warnst. and *S. squarrosum* have morphological variants tied to the Arctic (Flatberg, 2013). For instance a genetic study of *S. warnstorfii* revealed that its Arctic morph represents a genetic variant tied to the Arctic (Yousefi et al., 2019), while morphological and genetic analysis of *S. fimbriatum* Wilson established its Arctic morph as a separate species, *S. concinnum* (Berggr.) Flatberg (Flatberg, 2007; Shaw et al., 2012).

Sphagnum squarrosum on Svalbard, hereafter the Arctic morph has a more distinct yellow-brown colouration, a brown stem, and branch leaves that are unmistakably less squarrose than those observed in *S. squarrosum* growing elsewhere (Flatberg, 2013), hereafter the Boreal morph (Figure 1). The Arctic morph of *S. squarrosum* is even more laborious to distinguish from *S. teres* than the Boreal morph (Flatberg, personal communication).

Previous works on *S. squarrosum* have been concentrated on genetic structure within the Boreal morph in Europe with few specimens of the Arctic morph included. Weak genetic structure across the European distribution of *S. squarrosum* has been demonstrated by Szövényi et al. (2006) and Szövényi et al. (2007). Szövényi et al. (2006) included no specimens from Svalbard but included a specimen from the Arctic Kola Peninsula which displayed a haplotype not seen in other specimens, while Szövényi et al. (2007) included two specimens from Svalbard but discovered no spatial genetic structure within the limited representation. To this date, the Arctic morph of *S. squarrosum* has not been genetically examined in context of species delimitation.

Historically the morphological species concept which only requires knowledge of an organism's phenotype, has been used in bryophyte delimitation. However, a strictly morphological approach to species delimitation can introduce biases when inferring the evolutionary history of species and genera. An example of this is the exploration of genetic variation across the distribution range of *S. magellanicum* Brid. (Kyrkjeeide et al., 2016b) which under further investigation with genetic, morphological and ecological data turned out to consist of three species (Hassel et al., 2018). Bryophytes have extremely reduced morphologies (Vigalondo et al., 2019), which can lead to too conservative species delimitation (Patiño & Vanderpoorten, 2018). Due to an over usage of the term "cryptic species" in bryophytes, it has been suggested that morphology-based species delimitation should be carried out taking phylogenetic relationships among species into consideration (Renner, 2020). The phylogenetic species concept delimits species through the level of relatedness and requires molecular data. The latter have become increasingly accessible in recent decades (Gutiérrez & Garbino, 2018; Rieppel, 2010) but there are more concepts that add great value to determine a good species. The ecological species concept requires information about the location and habitat type of the different populations of an assumed species (Winston, 1999), and can be of great aid when it is used along with other species concepts (Shaw & Goffinet, 2008).

In fact, integrative taxonomy – using multiple species concepts and diverse methods when delimiting species – decreases the chance of any one source providing a data bias, and gives more stable taxonomic units in species delimitation (Padial et al., 2009). Integrative taxonomy also has the advantage of covering more needs as e.g., a strictly phylogenetic approach is of little help in the field, and a strictly ecological approach would be problematic in ecotones. A mixed approach utilizing morphology, ecology and genetic analyses successfully resolved the uncertainties of *S. magellanicum* induced by analysis done on genetic data alone (Yousefi et al., 2017), delimiting *S. medium* Limpr. and *S. divinum* Flatberg & K. Hassel from *S. magellanicum* (Hassel et al., 2018). Integrative taxonomy provides good results, therefore I will use this approach in my study of the Arctic and Boreal morph of *S. squarrosum*.

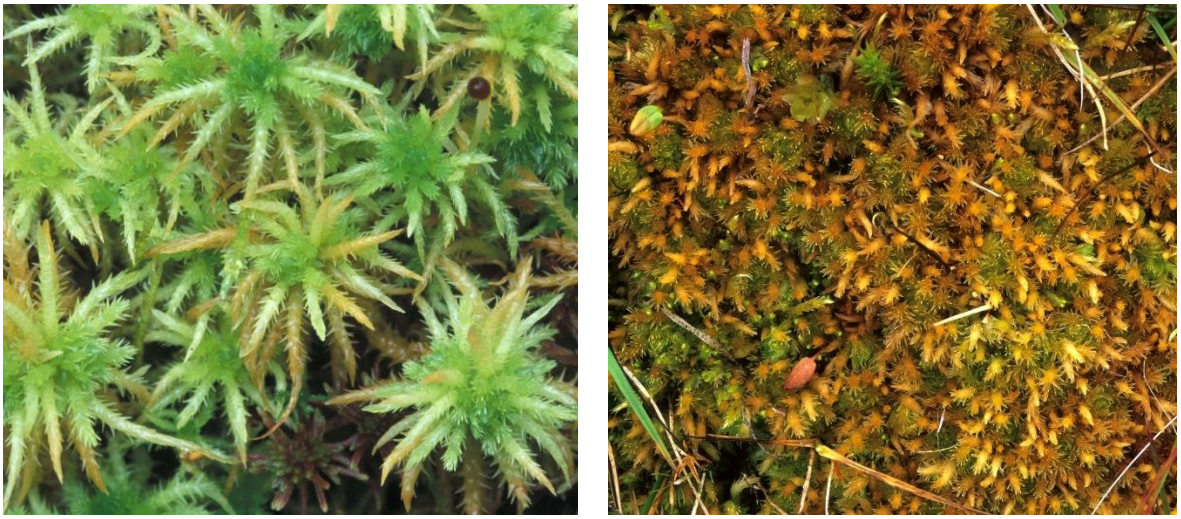

Figure 1: To the left: Boreal morph of S. squarrosum. To the right: the Arctic morph of S. squarrosum. Photo credit and identification: Kjell Ivar Flatberg

Aims

The aim of this study is to clarify the taxonomic status of the Arctic morph of *S. squarrosum* using an integrative taxonomic approach. I will use a common garden experiment and genomic data gained with RADseq, incorporating both the morphological and the phylogenetic species concept to explore whether the Arctic morph is a separate species or a phenotype. Specifically, I aim to (1) explore genetic distinctiveness of the Arctic morph and the Boreal morph of *S. squarrosum*, as well as (2) explore their relationship with *S. teres*, and *S. tundrae* Flatberg which co-occur with the Arctic morph of *S. squarrosum* on Svalbard. Lastly, I will (3) discuss possible demographic scenarios for *S. squarrosum*.

Material and methods

Sampling

In total, 21 samples of *S. teres*, 12 samples of *S. tundrae* in addition to 27 samples *S. squarrosum* from Norway, Finland, Greenland, Iceland, Faroe Islands, Russia, and Estonia, were extracted from the Trondheim herbarium (TRH) (Table 2 in Appendix). In addition, 54 samples of *S. teres*, *S. tundrae*, and *S. squarrosum* were collected on Svalbard, with vouchers deposited in TRH (Table 2 Appendix). Of these, Forty-four Specimens were dried at room temperature for use in DNA extraction, while 10 specimens were kept moist at 4 °C for use in the common garden experiment. Artskart (Artskart.artsdatabanken.no, 2019) was used along with Maps at TopoSvalbard (Norwegian Polar Institute, 2019) to locate possible sampling locations. Sampling of fresh material was carried out on Spitzbergen from the 19th to the 24th of August 2019. Samples of *S. squarrosum* collected north of the Arctic circle along with southern Greenlandic samples were defined as the Arctic morph. Four additional samples for the common garden experiment were collected from Boreal mires i.e., Momyra and Postmyra in Klæbu, mainland Norway, two of which were *S. squarrosum* and the other two *S. teres* (Table 2 in Appendix).

Common garden experiment

To test whether the morphological features e.g. colouration and squarosity of the leaves found in the Arctic morph is a result of environmental factors or an expression of genetically fixed morphology, a common garden experiment was conducted. The experiment included a total of 49 transplants consisting of: 1 sample of *S. tundrae*, 4 samples *S. teres*, 2 samples of *S. squarrosum* Boreal morph, and 7 samples of *S. squarrosum* Arctic morph. Samples were collected on Svalbard in August 2019 and stored moist and cool, and in Trøndelag in September 2019. See **Error! Reference source not found.**1 and 2 in Appendix for details and number of duplicates per sample. The experiment was performed at NTNU Vitenskapsmuseet over the course of three months with a light intensity of 90 ± 21 (SD) µmol·m -2·s-1 16 hours a day at 16°C during the day, and 12°C at night. The plants were placed intermixed in a seed nursery tray (Figure 2) half submerged in mire water collected at the minerotrophi Postmyra, Trøndelag. The water level was kept constant, and a clear plastic board was placed slightly suspended above the plants to reduce the risk of the desiccation by airflow from the climate control machine.

Figure 2: Common garden experiment at the day of assembly. Red triangle marks S. teres, yellow triangle marks S. tundrae, blue triangle marks the Boreal morph of S. squarrosum, and the blue circle marks the Arctic morph of S. squarrosum.

DNA extraction and RADseq library preparation

In total, 21 samples of *S. teres*, 12 samples of *S. tundrae* in addition to 27 samples *S. squarrosum* from Norway, Finland, Greenland, Iceland, Faroe Islands, Russia, and Estonia, were extracted from the Trondheim herbarium (TRH) (Figure 3, Table 2 in Appendix). In addition, 10 samples of S. teres, 10 samples of *S. tundrae*, and 14 samples of *S. squarrosum*, in total 34 samples, were collected on Svalbard with vouchers deposited in TRH all of which were dried at room temperature. Some sample locations overlapped for specimens used in genomic analysis and for specimens used in the Common Garden experiment, more details are available in Table 1 and 2 in Appendix. DNA from 34 samples of *S. squarrosum*, 18 of which were the Boreal morph and 16 of the Arctic morph, along with 25 samples of *S. teres*, and 16 samples of *S. tundrae*, in total 75 samples (**Error! Reference source not found.**1, Appendix) was extracted from dried capitulum tissue using the E.Z.N.A.®HP Plant DNA Mini Kit (Omega Bio-tek, Norway) with minor changes to the protocol provided by the

manufacturer. DNA concentration was measured using the Qubit 2.0 fluorometer (Thermo Fisher Scientific, USA) with the Qubit High Sensitivity kit (Thermo Fisher, Norway).

The DNA concentration of the samples was normalized to 130 ng, and Double digest Restriction-site Associated DNA sequencing (ddRADseq) genomic libraries were prepared for all samples. RADseq utilizes reduced-representation sequencing, which sequences a subset of coding and noncoding regions from the genome. RADseq provides a greater depth of coverage per locus sampled than available with whole genome sequencing methods for a lower cost (Andrews et al., 2016). RADseq has been successfully used to study genetic structure, phylogeography and evolutionary history in *Sphagnum* with greater depth than previously achieved (Duffy et al., 2020; Yousefi et al., 2017; Yousefi et al., 2019). The ddRADseq library build was carried out according to Westergaard et al. (2019) using the restriction enzymes EcoRI and TaqI with the following changes. During the adapter annealing, the heatblock was turned off after incubation at 98ºC for 2.5 min to ensure a slow cooling to room temperature. Samples were cooled to room temperature at a rate of 0.1°C/Sec during ligation. During pooling and size selection, 0.45x and 0.2x ratio of undiluted AMPure beads was used at the first and the second purification steps, respectively. The libraries were pooled together, quality checked using the Qubit 2.0 fluorometer (Thermo Fisher Scientific, USA) and the Agilent 4200 TapeStation system (Agilent, USA), and sequenced at The Norwegian Sequencing Centre (Oslo, Norway) using ½ lane on HiSeq4000 in 150 bp pair-end mode.

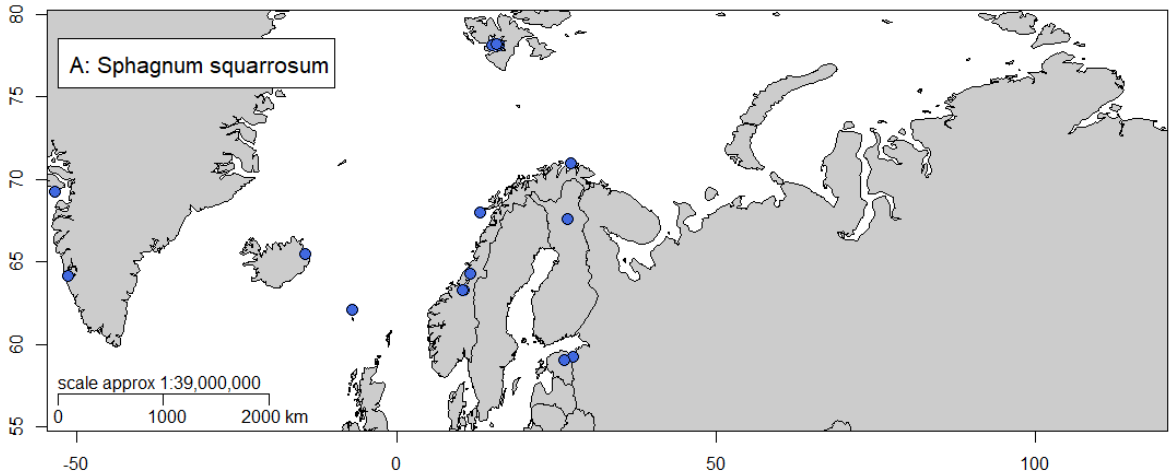

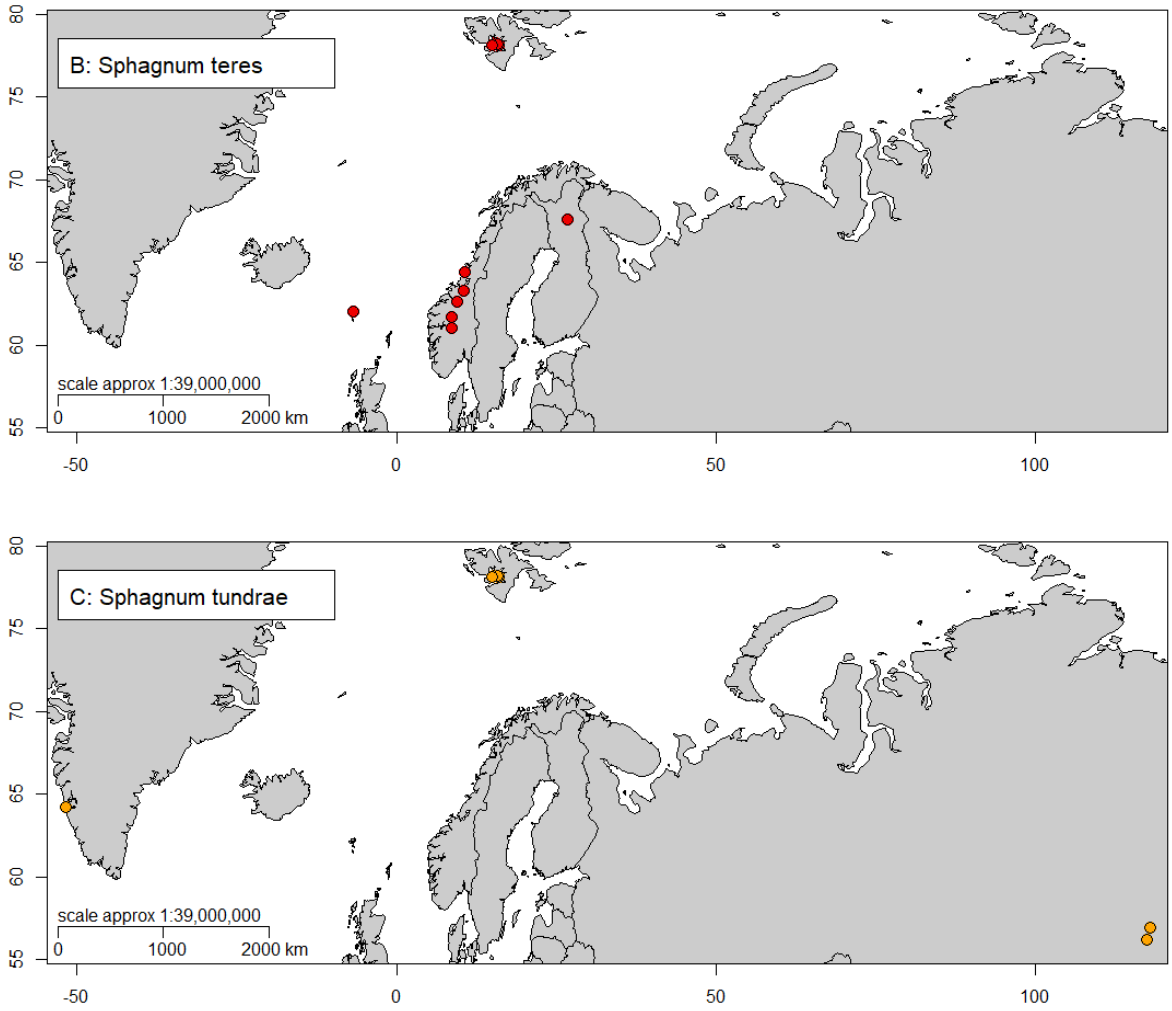

Figure 3: Locations of the accessions included in genetic analysis. Species are shown in the top left corner.

Sequencing data processing

The pipeline software Stacks v2.55 (Catchen et al., 2011) was applied to conduct a reference based analysis of the sequences. The 'process_radtags' module of Stacks was used on the raw sequencing reads to demultiplex, remove any read with an uncalled base, and discard reads with an average Phred score below 10 (Ewing & Green, 1998). The reads were aligned to a draft reference genome assembly of *Sphagnum angustifolium* (v0.5, DOE-JGI, http://phytozome.jgi.doe.gov/) using BWA with the 'mem' algorithm (Li & Durbin, 2009).

In addition, raw reads were aligned to the mitochondrial genome sequences of *S. squarrosum* (GenBank accession code KU725506.1) in the same manner as described above. A consensus sequence from aligned reads was created for each sample in ANGSD

(Korneliussen et al., 2014) using the effective base depth (-doFasta 3) approach (Wang et al., 2013) with a depth filter of minimum 30. The sequences were used for phylogenetic analysis.

SNP calling and filtering

The reads aligned to the nuclear genome were used to call variants using two pipelines in parallel. In the first pipeline, the 'gstacks' module of Stacks was used specifying the single nucleotide polymorphisms (SNP) model, setting minimum mapping quality to 20 to consider a read, and discarding unpaired reads. The 'populations' module of Stacks was run to export the SNPs present in at least 50% of the samples. Finally, the VariantFiltration module of GATK v4.1.9.0 (Auwera & O'Connor, 2020) was run to remove the few heterozygous sites in the haploid genome as these were presumed to be false since *S. squarrosum* is haploid. In the second pipeline, the variants were called using the 'HaplotypeCaller' module of GATK setting the minimum base quality required for calling to 20 and, the minimum mapping quality to 30, excluding soft clipped bases, and setting the ploidy to one as all the study species are haploid. Then the 'SelectVariants' module of GATK was run to extract SNPs, and the 'VariantFiltration' module of GATK was run with recommended parameters (Auwera et al., 2013) to remove low quality SNPs.

Both nuclear datasets were processed with VCFtools (Danecek et al., 2011) to create final datasets with a minimum depth per individual of 10, maximum depth of 50, maximum number of missing data per site at 50%, excluding all invariable sites and individuals with over 98% of missing data. Unbalanced population sizes can introduce biases in F_{ST} and STRUCTURE analysis (Wang, 2017) which is why a higher percentage of missing data was allowed in the genetic analyses. By including samples with more missing data, populations in this study were kept balanced as DNA was strenuous to extract from herbarium samples which led to the exclusion of many non-Svalbard samples before sequencing leaving these populations smaller from the beginning. For use in STRUCTURE and principal component analyses, one SNP per 500 bp was extracted with VCFtools to create thinned datasets to prevent physical linkage between the SNPs.

Principal Component Analysis and genetic differention

The R statistical environment v3.6.1 (R-Core-Team, 2019) was utilized to perform a Principal Component Analysis (PCA) on the thinned nuclear datasets from both pipelines

using the ‘adgenet’ v2.1.3 package (Jombart & Ahmed, 2011) to identify genetic clusters, and the ‘vcfR’ v1.12.0 package (Knaus & Grünwald, 2017) to load VCF files. The results of the analyses using both datasets were nearly identical, as expected (Wright et al., 2019). Therefore, the dataset generated with Stacks henceforth called the nuclear dataset, was utilized for further analysis. A measure of pairwise interspecific genetic differentiation, F_{ST}, was calculated with the ‘populations’ module of in Stacks.

STRUCTURE analysis

To determine the presence of any genetic structure in the data, STRUCTURE v2.3.4 (Pritchard et al., 2000) was used on the nuclear dataset. The analysis was run testing K=2 to K=4 with a burnin of 50,000 and 100,000 subsequent iterations, assuming correlated allele frequencies among populations as suggested by Pritchard et al. (2000) and no admixture. An additional analysis was run separately for *S. squarrosum* with the same parameters as above testing *K*2 to *K*4. The StructureSelector server was utilized for postprocessing of the results (Kopelman et al., 2015).

Phylogenetic analysis

Concatenated multiple sequence alignment in fasta format was generated from the nuclear dataset using the method described in Meleshko et al. (2021). Two species, *S. lindbergii* Scimp. and *S. compactum* Lam. & DC., were used as outgroups. For that, concatenated multiple sequence alignment for samples AI9 and NJ210 was obtained from the filtered SNP dataset by Meleshko et al. (2021) in the same manner. RAxML v8.2.12 (Stamatakis, 2018) was run with 100 bootstrap replicated with the GTRGAMMA model, inferring phylogenetic relationships under maximum likelihood. The mitochondrial dataset and the nuclear dataset were run with the same parameters along with an additional RAxML run using a subset of the nuclear dataset that included *S. squarrosum* samples and two *S. tundrae* samples from Svalbard as outgroups. FigTree (Rambaut, 2018) was used to edit and view the maximum-likelihood phylogenetic trees inferred with RAxML.

Results

Common garden experiment

Throughout the three months of the common garden experiment, the Arctic and Boreal morphs kept their differences i.e. yellow-brown pigmentation and only partially squarrose leaves on the divergent branches of the Arctic morph, and green colour and clearly squarrose leaves on the divergent branches of the Boreal morph. One change that we did observe was that the Arctic morph was approaching the Boreal morph in growth form, i.e. going from a compact growth form to a more loosely arranged shoots. Appearance of samples on final day of experiment shown in Figure 4 and Figure 5.

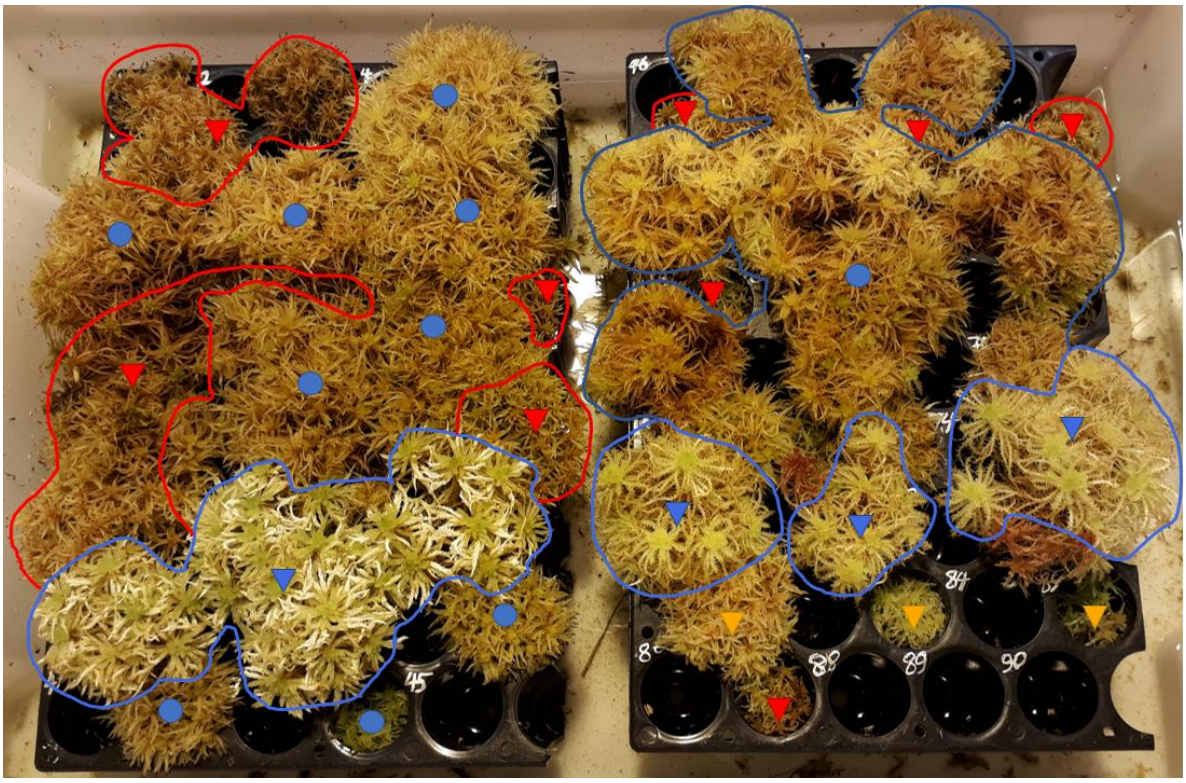

Figure 4: Common garden experiment, day of dismantling. Red triangle marks S. teres, yellow triangle marks S. tundrae, blue triangle marks the Boreal morph of S. squarrosum, and the blue circle marks the Arctic morph of S. squarrosum. Lines have been added where distinguishing species is challenging.

Figure 5: The Arctic morph of S. squarrosum to the left, compared to the Boreal morph of S. squarrosum to the right on the final day of the common garden experiment. Differences in morphology were still apparent.

SNP calling and filtering

A mean of 1,947,715 reads per sample were mapped with BWA, with a mean of 1,507,007 reads per sample properly paired.

After excluding 17 samples with >98% of missing data, the nuclear dataset contained 40,766 SNPs with a mean number of SNPs of 25,649 per sample (Figure in Appendix), a mean depth per sample of 24.34, and a mean percentage of missing SNPs of 37.08% per sample. The thinned nuclear dataset contained 6,175 SNPs. The final dataset contained 56 samples and 5 duplicates, 17 samples were *S. teres*, 12 were *S. tundrae*, and 27 *S. squarrosum* (13 were the Boreal morph, and 14 were the Arctic morph) (**Error! Reference source not found.**1 in Appendix).

The *S. squarrosum* samples had a mean of 13,497 SNPs ranging from 731 to 39,543 SNPs, and a mean of 30% missing data. The *S. teres* samples had a mean of 6,947 SNPs ranging from 1,555 to 38,280 SNPs, and a mean of 42% missing data. The *S. tundrae* samples had a mean of 4,742 SNPs ranging from 1,175 to 36,297 SNPs, and a mean of 45% missing data.

Genetic structuring

In the PCA, the first three Principal Components (PCs) accounted for 72.33% of the variation (Figure 6). PC1 accounted for 52.56% of the variation, and separated the Boreal and the Arctic morph of *S. squarrosum* from *S. teres* and *S. tundrae*. PC2 accounted for 13.87% of the variation, and separated *S. tundrae* from *S. teres* (Figure 6A). Several samples cluster close to the origo that correspond to the samples with over 90% missing data. The PC3 explained 5.90% of the variation, and distinctly separated all the samples from Norway and Faroe Islands from the rest (Figure 6B). There was a slight difference in the positioning of the remaining samples where the Arctic morph placed higher on the Y-axis but this was not a consistent pattern.

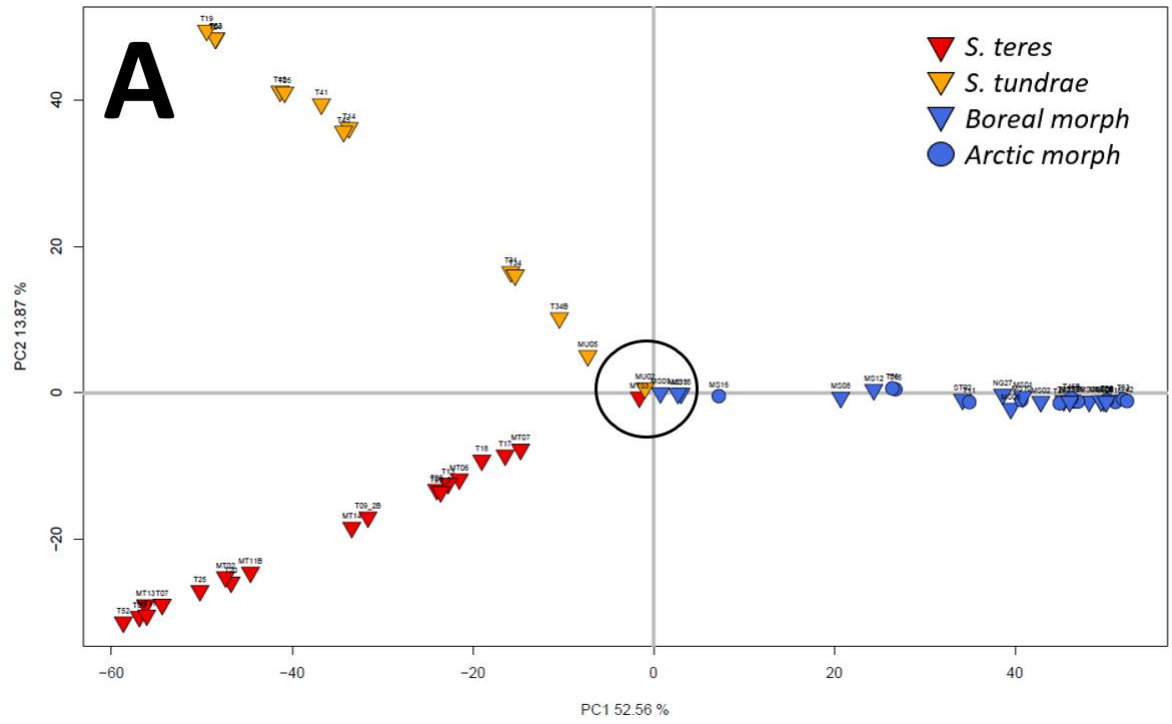

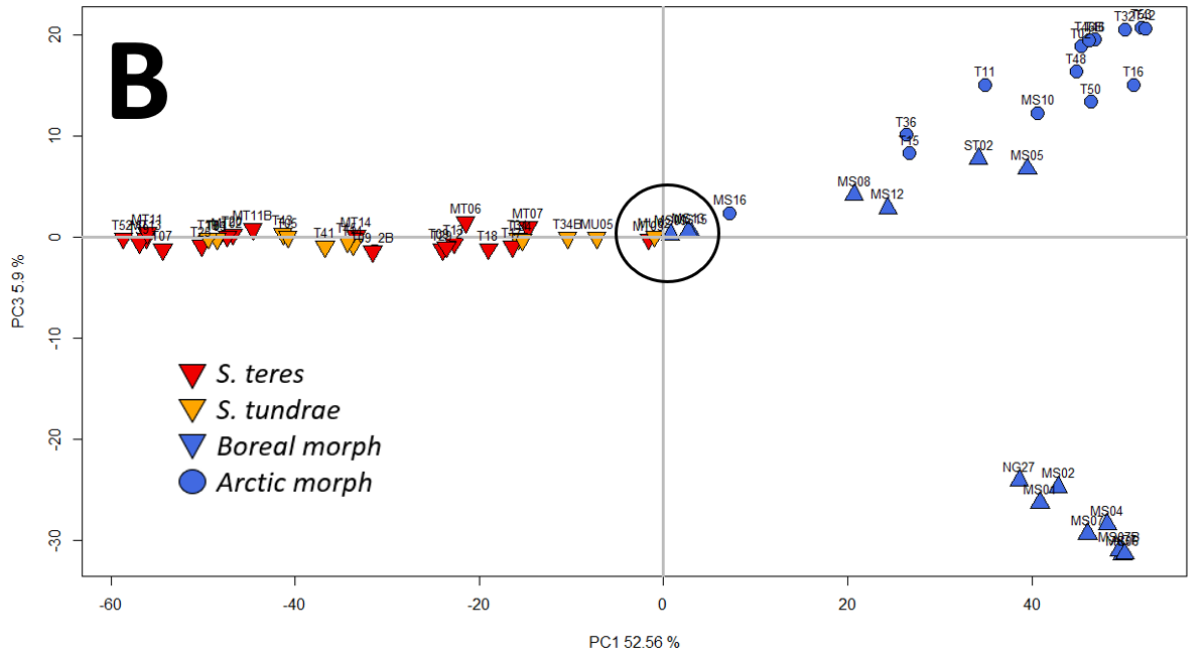

Figure 6: Principal Component Analysis blue shows the morphs of S. squarrosum, within the black circle are the samples with more than 90% missing data. ***A****: PC1 and PC2, point colour and shape represent population as shown in top right corner.* ***B****: PC1 and PC3, point colour and shape explanation is in bottom left.*

In the STRUCTURE analysis, the best supported *K* was four according to ΔK (ΔK=2575.44), Δ*K* for other *K*s were below 1. Δ*K*=4 showed differentiation among *S. teres*, *S. tundrae* and *S. squarrosum* (Figure 7) but no differentiation between the morphs within *S. squarrosum*. The analysis revealed that the Arctic morph belongs to the same genetic cluster as the Boreal morph of *S. squarrosum* (Figure 7). An emerging intraspecific genetic substructure in *S. squarrosum* is visible in *K*=3 where samples from Faroe Island and South Norway are separated from the rest of the *S. squarrosum* samples. There seems to be more admixture between samples from Finland, Iceland, Estonia and Greenland and other samples of the Arctic morph from Arctic areas than between these samples and the Faroe Island and South Norway.

In the analysis of *S. squarrosum*, the best supported *K* was four according to Δ*K* (Δ*K*= 51.14). The pattern emerging in the analysis including all study species was detectable in the analysis with only *S. squarrosum* as well. In the major cluster for *K*=2 (Figure 8), samples from Faroe Island, and South Norway cluster separately from the rest of the samples (Figure 9) which is in concordance with the emerging clustering of these populations in the minor cluster of *K*=6 for the analysis run with all species. In *K*=4 (Figure 8, Figure 9), three clusters are present despite there only being two morphs. Samples from Estonia, Finland, Iceland, and

Greenland seem to have more admixture with samples from Svalbard, Arctic Greenland and Arctic Norway than samples from South Norway and Faroe Islands. Some individuals from Svalbard, Faroe Island and South Norway seem to have some admixture between them visible in the admixture map on Figure 9.

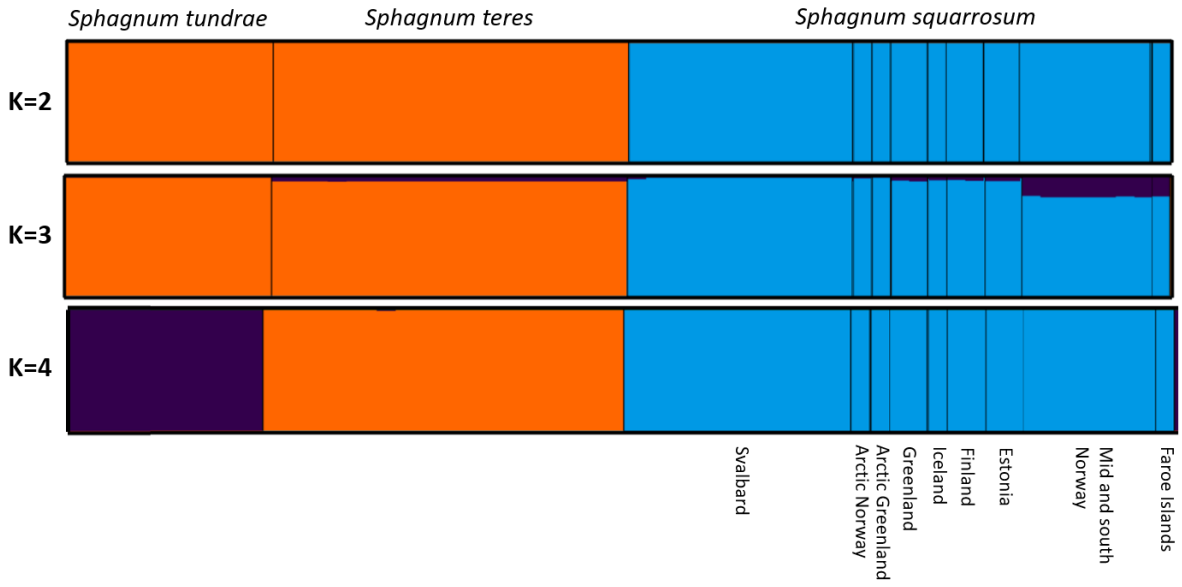

Figure 7: STRUCTURE diagram showing clusters for K 2-4. All groups titled with a country at the bottom belong to S. squarrosum.

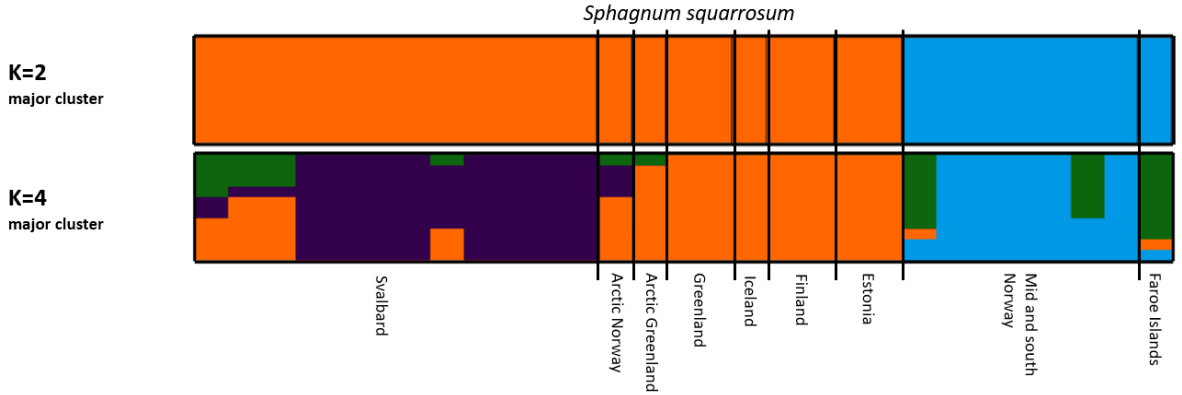

Figure 8: STRUCTURE diagram showing major clusters of S. squarrosum for K 2 and 4. Country of origin is marked at the bottom.

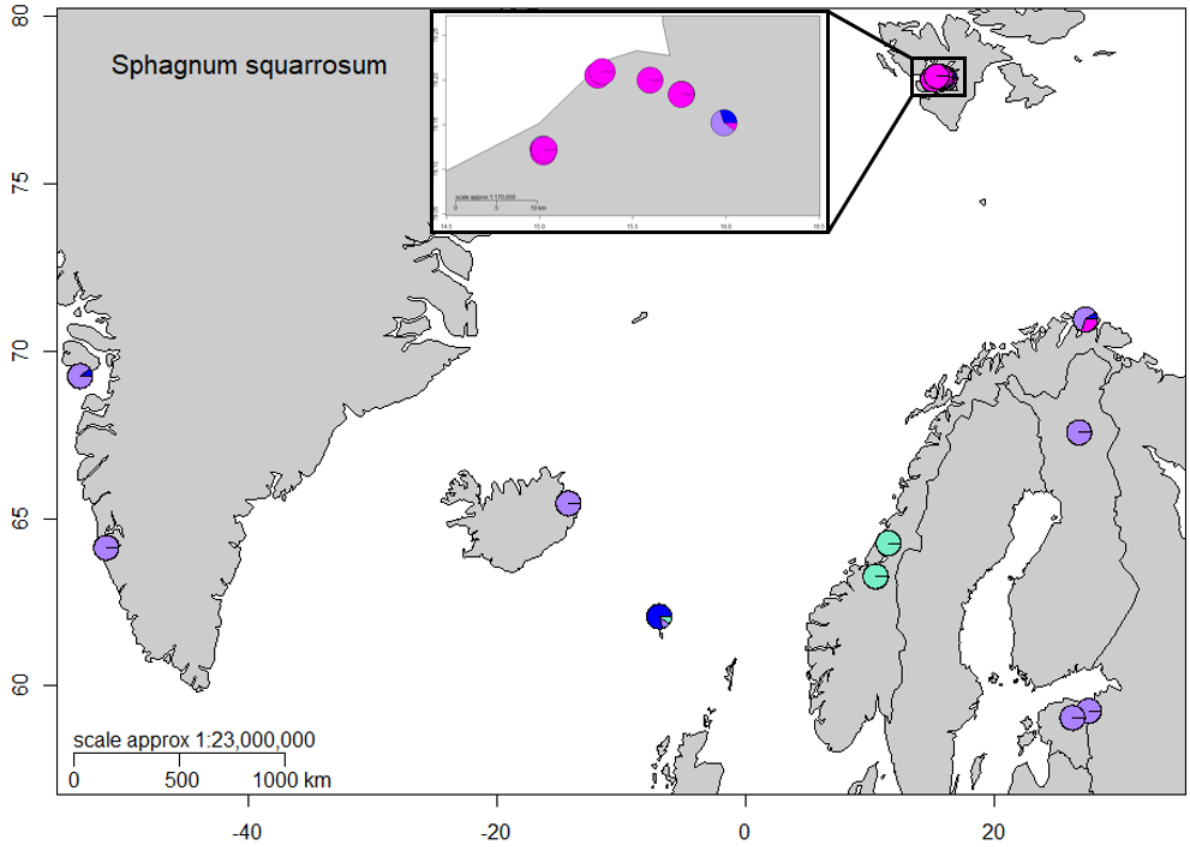

Figure 9: Admixture map showing S. squarrosum clustering of K=4 from the STRUCTURE analysis.

Phylogenetic analysis

RAxML inferred a fully bifurcating phylogeny with a monophyletic relationship between the Arctic morph and the Boreal morph of *S. squarrosum* with a high bootstrap support in both analyses (Figure 10, Figure 11). In the nuclear-based phylogeny (Figure 10), *S. squarrosum* formed a sister clade to *S. teres* and *S. tundrae* both of which were monophyletic with a high bootstrap value. There is geographic structure within *S. tundrae*, with samples from Russia and Svalbard forming separate, highly supported clades; this structure is not present in the mitochondrial-based phylogeny. In S. teres the non-Svalbard samples are inferred in three clades in the mitochondrion phylogeny (Figure in Appendix), but in two clades in the nuclear phylogeny, while the Svalbard samples are inferred to comprise two clades in both phylogenies but with differing placement relative to the non-Svalbard clades. *Sphagnum teres* is geographically structured in the nuclear phylogeny with Svalbard samples forming a polyphyletic group consisting of two clades, where the clade with the Svalbard samples and the Faroe Island sample has lower support than the clade with samples from Svalbard. In the mitochondrion-based phylogeny, *S. teres* also have two

moderately supported clades of the samples from Svalbard but the Faroe Island sample is inferred to be more closely related to the Norwegian samples than the Svalbard samples. However, the relationship between the Svalbard clades is incongruent between the phylogenies. In the nuclear phylogeny, the Svalbard clades are inferred as more closely related to each other than in the mitochondrial phylogeny.

The separate RAxML analysis of *S. squarrosum* inferred a topology identical to the full nuclear-based phylogeny (Figure 11). Three clades were detected, one of which is a highly supported branch holding all South Norwegian samples along with a sample from Faroe Islands referred to as the green group henceforth. The green group formed a sister clade to the remaining samples bifurcating into two highly supported monophyletic clades, one of which contained samples from Greenland, Finland, Iceland, and Estonia, this clade will be referred to as the blue group. The last clade contains all samples from Svalbard along with samples from Northern Norway and the northernmost part of Greenland, and will be referred to as the purple group and corresponds somewhat with the delimitation of the Arctic morph but excludes southern Greenlandic samples. The phylogeny of *S. squarrosum* inferred using the mitochondrial sequences (Figure , Appendix) also supported the monophyly of the green group but with lower support than inferred in the nuclear phylogeny. In the mitochondrial phylogeny the individuals from the purple and blue group are intermingled, lacking the well supported separation found in the nuclear phylogeny.

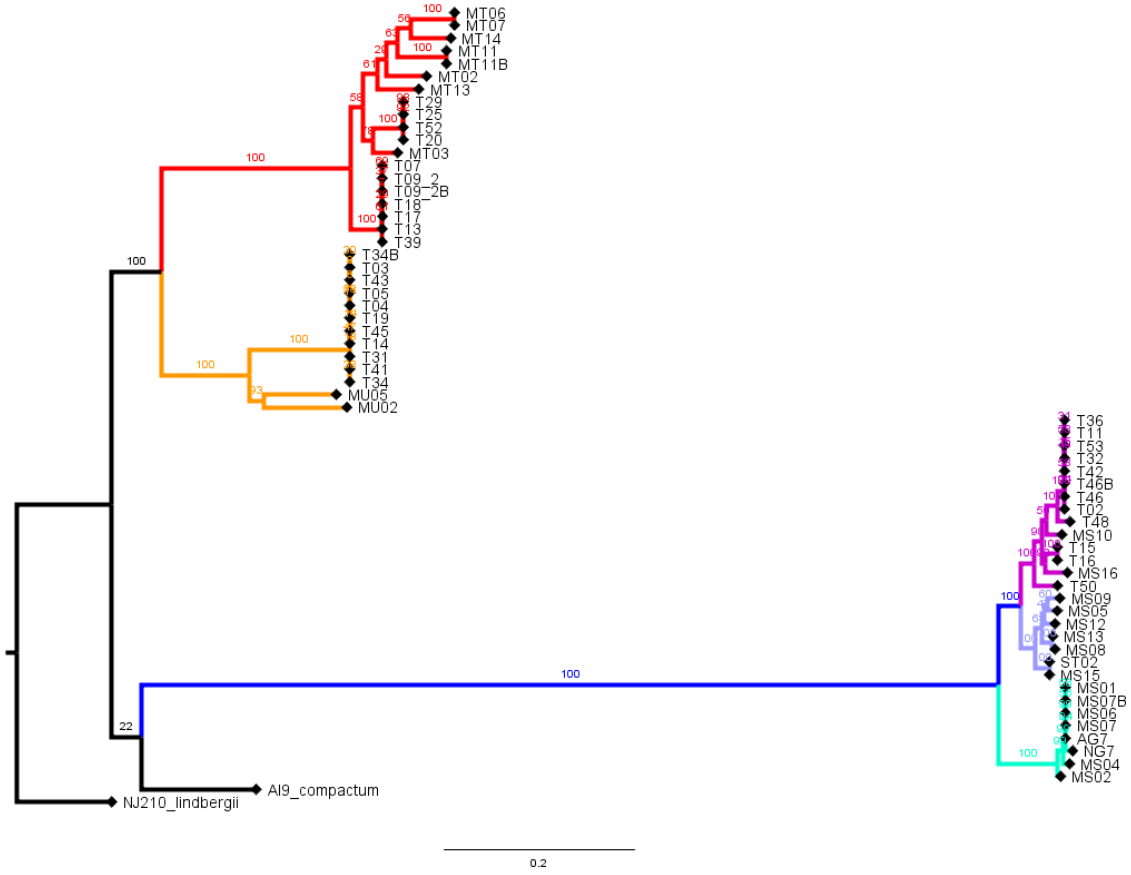

Figure 10: phylogram showing phylogenetic relationships inferred from the nuclear dataset by RAxML. Branch labels represent bootstrap values. Sphagnum teres is coloured red, S. tundrae is coloured yellow, and the branch holding S. squarrosum is coloured blue with the three main branches of S. squarrosum coloured according to their genetic groups named the purple, blue and green group.

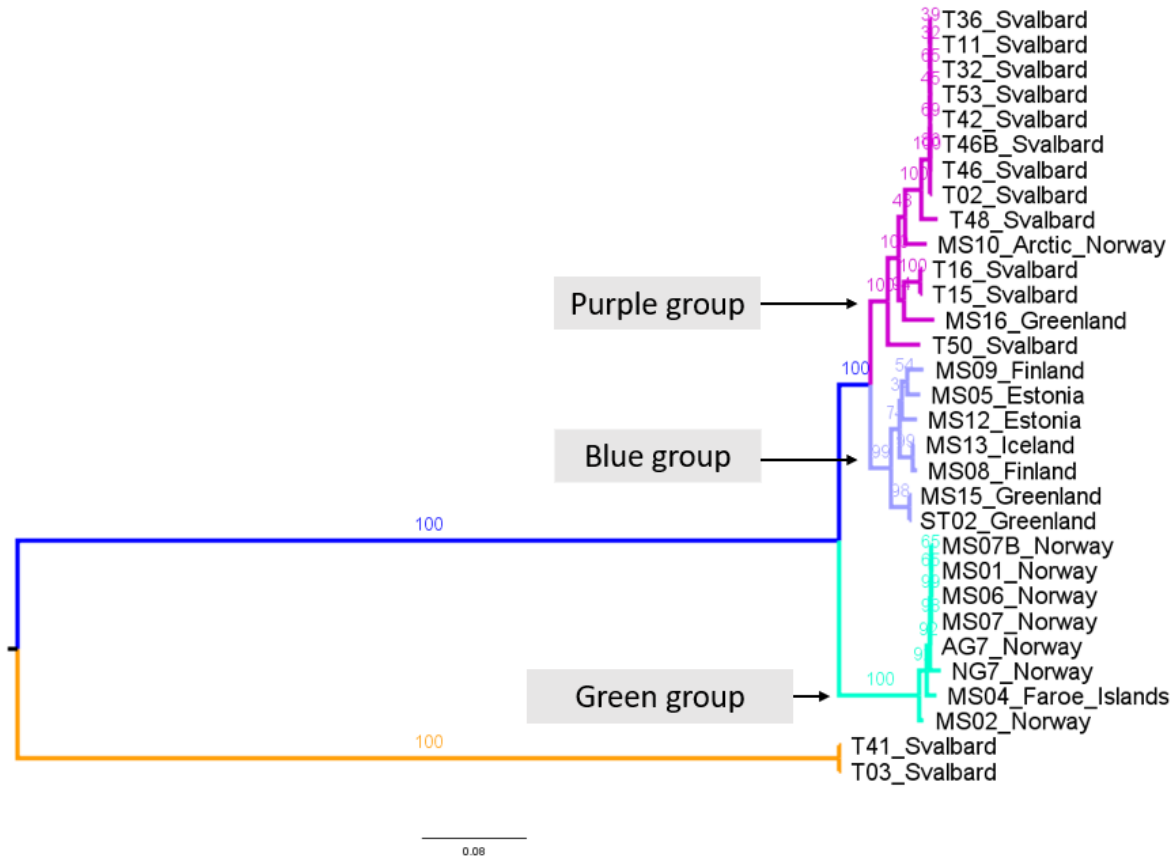

Figure 11: Phylogenetic relationships between S. squarrosum and two randomly chosen samples of S. tundrae as outgroups inferred from the nuclear dataset with RAxML. Branch labels represent bootstrap value and sample origin is to the right in grey. The two samples of S. tundrae are in orange. The three main branches of S. squarrosum have been named for convenience corresponding to the grey squares.

Genetic differentiation

The F_{ST} estimates (Table 1, **Error! Reference source not found.**) between *S. squarrosum*; and *S. teres* or *S. tundrae* are higher than that between *S. teres* and *S. tundrae* which is consistent with the results of the STRUCTURE analysis and PCA and suggests a that the species are genetically distinct with a high degree of genetic differentiation among them. Within *S. squarrosum* the lowest F_{ST} value is found between the purple and blue group (0.355), and the highest value is found between the green group and the blue group (0.753) which matches the pattern observed in the STRUCTURE analysis and indicates strong intraspecific genetic differentiation in *S. squarrosum*. The F_{ST} value between the purple group and the green group is 0.617, which almost twice that of the purple group and the blue group.

Table 1: Pairwise interspecific F_{ST} estimates (in bold), and intraspecific F_{ST} estimates between the morphs of S. squarrosum, and among the groups found in phylogeny of S. squarrosum. Populations size is in parenthesis.

	S. tundrae (12)	***S. teres*** (21)	*Arctic morph* (15)	*Purple group* (13)	*Green group* (7)
S. teres (12)	**0.655**				
Arctic morph (13)	**0.875**	**0.761**			
Purple group (15)	**0.893**	**0.773**			
Boreal morph (12)	**0.842**	**0.735**	0.391		
Green group (7)	**0.943**	**0.802**		0.617	
Blue group (7)	**0.927**	**0.770**		0.355	0.753

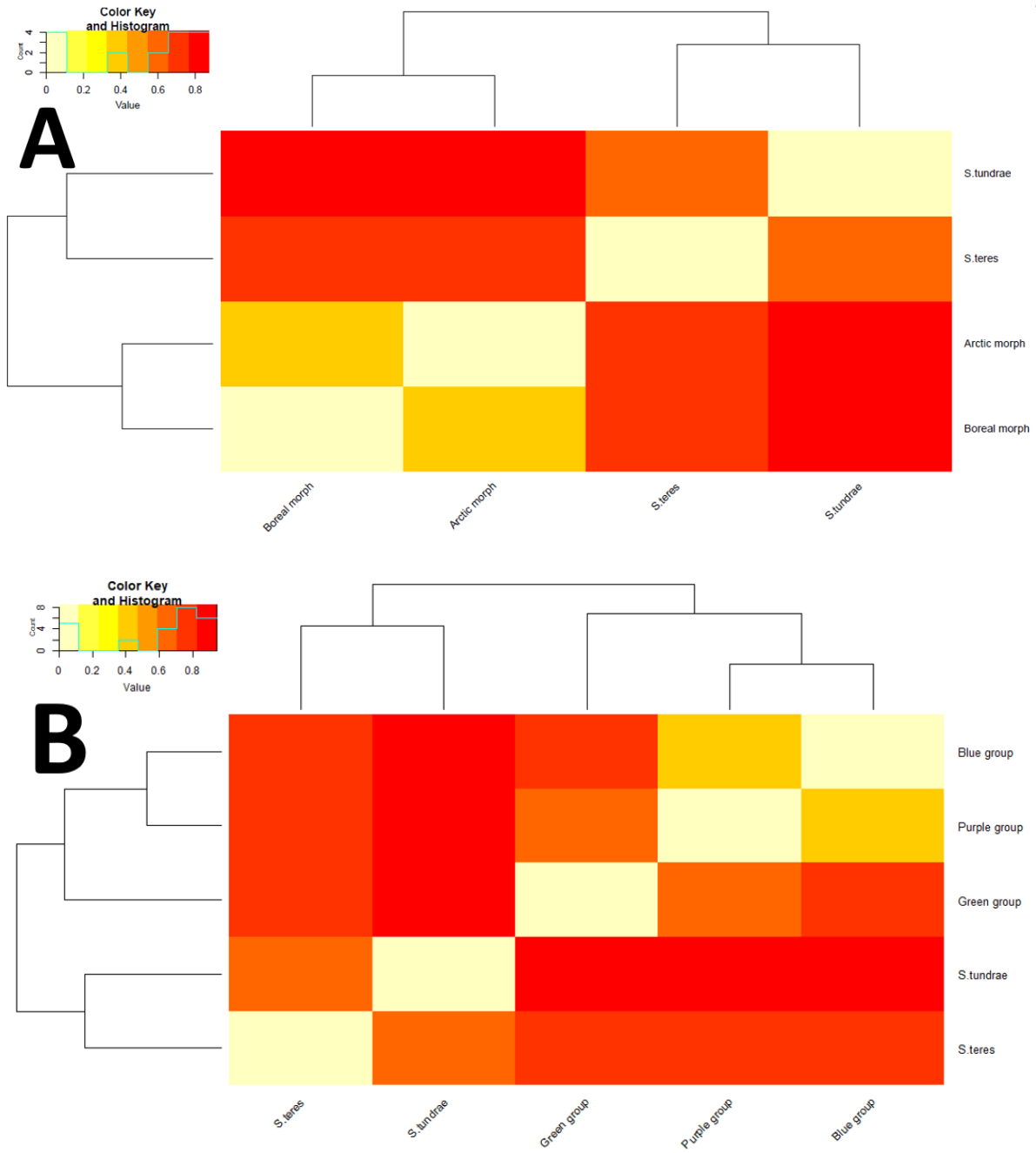

Figure 12: Pairwise F_{ST} estimates between S. teres, S. tundrae and the two morphs (A) and the genetic groups (B) of S. squarrosum. Colour key and histogram is presented in the left corner showing which colour the F_{ST} values are represented by.

Discussion

The molecular analyses taxonomically place the Arctic morph of *S. squarrosum* in a clade with the rest of *S. squarrosum s.l.* and suggests that the Arctic morph is not closely related to *S. teres* or *S. tundrae*. The common garden experiment does not yield any supporting evidence for this conclusion, however it does not support the Arctic morph belonging to the other study species either. Genetically, *S. tundrae* and *S. teres* seem to be more closely related to each other than to *S. squarrosum*. Russian samples of *S. tundrae* show strong differentiation from the remaining *S. tundrae* samples from Svalbard. Strong geographical structure was found in *S. squarrosum* separating it into two genetic groups that do not correspond with the two morphs defined in this thesis.

Taxonomic relationship between *S. squarrosum*, *S. teres* and *S. tundrae*

The genetic analyses highly supported the presence of three species in the dataset with no support of gene flow among them. Samples of the Arctic morph of *S. squarrosum* were inferred to be within *S. squarrosum* with unanimous support. F_{ST} values support a similar amount of genetic differentiation among groups of *S. squarrosum* as there is between *S. teres* and *S. tundrae*. The different genetic groups of *S. squarrosum* may warrant taxonomic recognition, however this would involve a morphological study of the genetic groups. The phylogenetic analysis highly supports a more recent common ancestor of *S. teres* and *S. tundrae* that is not shared by *S. squarrosum.*

In most of the analyses, Russian samples of *S. tundrae* displayed a high degree of genetic differentiation from the Svalbard samples of *S. tundrae*. The Russian samples of *S. tundrae* comprise a separate branch of the nuclear-based phylogeny with high bootstrap support. A clear signal of dissimilarity between the Russian and Svalbardian samples is evident in STRUCTURE as well, where Russian samples were separated from *S. tundrae* before *S. tundrae* was differentiated from *S. teres* (results not shown). F_{ST} values could not be computed to explore genetic differentiation between Svalbard and Russian samples as the Russian population only comprised two individuals. Svalbard is the type location of *S. tundrae* (Flatberg, 1994) so, presuming the Svalbard samples represent the holotype, the Russian samples of S. tundrae might comprise a currently undescribed taxon.

Spatial variation of *S. squarrosum*

The PCA, STRUCTURE, phylogenetic and F_{ST} analyses inferred strong geographic genetic structure within *S. squarrosum*. There is high support for two groupings in the genetic data, one consisting of the green group and the other combining the purple and blue group. This grouping conflicts with the phenotype groupings as most samples in the green and blue group represent the Boreal morph (except for two southern Greenlandic samples which belong to the Arctic morph), while the purple group contains most samples of the Arctic morph. A separation into two species corresponding to the Arctic morph and Boreal morph is not supported by my findings, but there seems to be more intraspecific genetic structure than previously found in *S. squarrosum* (Szövényi et al., 2007; Szövényi et al., 2006).

The morphs of *S. squarrosum* kept their respective morphologies throughout the common garden experiment, this could be an indication that the morphs of *S. squarrosum* are not conspecific according to the morphological species concept. The lack of phenotypic change seen in the morphs indicate that the morphological differences between them are phenotypic variation instead of plasticity. The differing phenotypes could be local adaptation, the genetic basis for this is largely supported by genetic analysis except for the discrepancies mentioned in the paragraph above. However, there was no in-depth morphological data collected other than the general appearance so any subtle morphological change during the experiment could have been overlooked. Another source of uncertainty around the results is the duration of the experiment since minimum time for observing a phenotypic change has not been established for *Sphagnum*. Growth experiments conducted on *S. magellanicum* have previously been terminated with conclusive results after six months (Yousefi et al., 2017) or 2 years (Schwarzer & Joshi, 2017). Therefore, it is possible that the period of 3 months used in this study was too short to conclude on the status of the morphological traits displayed by the Arctic morph on Svalbard.

The blue group was characterized by incongruent results in the phylogenetic analyses based on different markers and by a high proportion of missing data (Figure in Appendix), whereas the green group and purple group which had the least missing data produced the most consistent results. A high number of missing sites can introduce biases in RAxML (Izquierdo-Carrasco et al., 2011), this suggests that the placement of the blue group might have been affected by missing data in the nuclear dataset. Despite the unequal number of missing sites between samples of *S. teres*, the groups with many missing sites do not constitute a separate clade in the phylogenies. To keep a high sample size among sites and species, some missing

data was accepted. Missing data can introduce noise in PCA (Bailey, 2012) and lead to biases and an increased error rate, especially when missing data is skewed towards some groups (Brown et al., 2012). Missing data is somewhat accounted for in RAxML as well by its algorithm although it is not completely eliminated (Izquierdo-Carrasco et al., 2011).

The incongruence of the mitochondrial and nuclear could be due to differing evolutionary histories of the genomes (Burger et al., 2003). This difference could lead to inferring different geographical patterns and phylogenies based on which genome is chosen (Chong et al., 2016; Tsutsui et al., 2009). The mitochondrial genome is small compared to the nuclear genome of plants, in addition numerous mitochondria are found within each cell, increasing the possibility that the mitochondrial dataset is more complete than the nuclear dataset. Considering both phylogenies to be true, the green group remains highly supported while the blue and purple group could be more affected by incomplete lineage sorting. There is a higher number of markers in the nuclear dataset compared to the mitochondrial one, which could provide more support to the nuclear phylogeny compared to the mitochondrial phylogeny.

Estimates of intra- and interspecific genetic differentiation are available from other studies on *Sphagnum*, for example in the *S. recurvum* P. Beauv. complex where closely related species displayed lower F_{ST} values (Duffy et al., 2020) than the value found between the green group and other *S. squarrosum* samples. This could support a division of *S. squarrosum* into a green group and a group consisting of the Arctic and blue group. However basing species delimitation on F_{ST} values of another subgenera would contribute to faulty delimitation as F_{ST} values are not a direct measure of important aspects of speciation such as reproductive isolation. The F_{ST} values between the two morphs of *S. magellanicum* later separated into *S. medium* and *S. divinum* (Hassel et al., 2018) were somewhat higher (Yousefi et al., 2017) than the value between the green group and the rest of the *S. squarrosum* samples. However, Yousefi et al. (2019) found F_{ST} values in *S. warnstorfii* that were higher than the value between the green group and the other *S. squarrosum* samples, and did not separate their groups into taxa because of discrepancy between morphological and molecular data regarding the placement of the split. Combined, this provides weak support for delimiting the green group into a separate species.

No spatial structure was found in North-Western European *S. squarrosum* based on chloroplast markers (Szövényi et al., 2006), this differs from the results of my study. Some

sampling locations of their study overlap with locations in my study so the same populations might have been sampled. The Arctic sample included in their study had an exclusive haplotype, the similarities of the results strengthens the finding of genetic structuring within *S. squarrosum*. Another study by Szövényi et al. (2007) included four samples from the Arctic, three of which correspond to sampling locations in this study and some displayed exclusive haplotypes. Perhaps utilizing RADseq with their sampling regime would find a gradient of haplotypes across Northern Europe, explaining their lack of distinctiveness in Norwegian samples (Szövényi et al., 2007; Szövényi et al., 2006) while explaining my distinctiveness by failure to sample the whole gradient. However the difference between their studies and mine could be a matter of genomic sampling as they included three genomic regions each (Szövényi et al., 2007; Szövényi et al., 2006) and my study is based on a plethora of widespread SNPs gained with RADseq.

A more widespread sampling regime using RADseq could be the key to the most sturdy conclusion. Such a dataset could answer if there are any other localities that belong in the groups found in my study, or as previously mentioned, if the groups found in this study are fragments of a continuous gradient rather than separate units. A sampling regime that extends to North America would allow exploring whether there are transatlantic groups that correspond to the groups found in Europe.

Biogeography of S. squarrosum

The spatial genetic structure detected in *S. squarrosum* resembles the genetic structure detected in studies of other species in the genus. A study on *S. warnstorfii* detected genetic groupings consisting of an Arctic and a Boreal group which were inferred to have separated before the last glacial maximum (LGM) (Yousefi et al., 2019). In *S. fimbriatum* Svalbardian specimens formed a divergent clade which could have had its LGM refugia on the northern coasts of Eurasian Russia before dispersing to Svalbard (Szövényi et al., 2006). The purple group of this study contains most of the Arctic samples, although it does not encompass all the specimens of the Arctic morph. Still the genetic differentiation between groups of *S. squarrosum* in this study could indicate that the groups survived the LGM in two or perhaps three separate refugia. It is possible that the purple group of *S. squarrosum* shared a refugia with the Arctic groups of *S. warnstorfii* and *S. fimbriatum*. Due to the shared habitat preference, it is possible that the Arctic morph shares phylogeographic patterns with *Rubus*

chamaemorus L. (Ehrich et al., 2008) which survived the LGM in refugia in Beringia (Elias et al., 1997) and Siberia before it colonized Svalbard (Ehrich et al., 2008).

There is no record of spore production in *Sphagnum* within nearly 1,000 km of Svalbard (Sundberg, 2013) which would make dispersal to available habitats within Svalbard slow as it would need to be through asexual reproduction. However, spore deposition has been recorded from the outside which enables quick dispersal and establishment on the archipelago (Sundberg, 2013). Probable vectors are wind, animals (Neilson et al., 2005), drift wood and drifting sea ice (Alsos et al., 2016), out of these vectors animal dispersal (Lewis et al., 2014) and dispersal by drifting sea ice (Nordal, 1987) has been recorded for bryophytes, as well as wind dispersal in *Sphagnum* (Sundberg, 2013) along with other bryophytes (Vanderpoorten & Goffinet, 2009). When the wind travels from Greenland to Svalbard in July, it is too early for spore capsules to be ripe in the cool climate of the region (Flatberg, 2007) which makes Greenland an improbable spore source for Svalbard. In a study exploring the genetic pattern of 9 vascular plant species in the Arctic, it seems that the most prominent source of migrants to Svalbard is North-western Russia (Alsos et al., 2007) so the Arctic morph could have a similar origin. A more extensive sampling regime of Arctic areas and morphological studies are needed to draw any conclusions on the origin of the genetic distinctiveness of the purple group.

The genetic structure within the Boreal morph could be a result of separate origins of the genetic groups. Pinpointing locations of refugia is beyond the scope of this study as *Sphagnum* has a great dispersal capacity and the sampling of this study is limited to Northern Europe. The Atlantic Ocean is a weak barrier to gene flow in *Sphagnum* while terrestrial terrain seems to pose more of a barrier (Kyrkjeeide et al., 2016a) which could explain the separation of the genetic groups within Europe.

Future perspectives

Further research efforts on *S. squarrosum* should be directed towards discovering the context of the genetic structure found in North-Western Europe in this study. A widespread sampling regime would shed light on transatlantic spore dispersal according to which populations group together. Information on spore dispersal in the Northern hemisphere would enable predictions on the number of migrants expected on each side of the Atlantic, which would allow us to acquire knowledge on expected genetic diversity. Climate change puts increasing pressure on natural populations, which genetic diversity helps mitigate, therefore information on the frequency and routes of spore dispersal would ensure the knowledge to make the right conservation decisions (Dewoody et al., 2021). The Arctic morph and purple group should receive special attention in this endeavour with a special focus on genetic diversity exclusive to the Arctic as the Arctic is warming at an increased rate compared to the rest of the world (IPCC, 2021). The *S. tundrae* samples from Arctic Russia should also receive academic attention as they could constitute a separate species, and currently there is no information to indicate the spatial variation of the genetic variation in these specimens. Reconstructing the demographic histories of *S. squarrosum* and *S. tundrae* would not only aid conservation efforts specific to these species but could also provide knowledge of the dispersal and speciation mechanisms in non-vascular plants.

References

Alsos, I. G., Ehrich, D., Seidenkrantz, M.-S., Bennike, O., Kirchhefer, A. J., & Geirsdottir, A. (2016). The role of sea ice for vascular plant dispersal in the Arctic. *Biology Letters, 12*(20160264).

Alsos, I. G., Eidesen, P. B., Ehrich, D., Skrede, I., Westergaard, K., Jacobsen, G. H., Landvik, J. Y., Taberlet, P., & Brochmann, C. (2007). Frequent Long-Distance Plant Colonization in the Changing Arctic. *Science Reports, 316*(5831), 1606-1609.

Andrews, A. L. (1913). Notes on North American *Sphagnum*. V (Concluded). *The Bryologist, 16*(5), 74-76.

Andrews, K. R., Good, J. M., Miller, M. R., Luikart, G., & Hohenlohe, P. A. (2016). Harnessing the power of RADseq for ecological and evolutionary genomics. *Nature Review Genetics, 17*, 81-92.

Artskart.artsdatabanken.no. (2019). Retrieved from https://artskart.artsdatabanken.no/app/#map/526512,8690616/7/background/greyMap/filter/%7B%22TaxonIds%22%3A%5B188851%5D%2C%22IncludeSubTaxonIds%22%3Atrue%2C%22Found%22%3A%5B2%5D%2C%22NotRecovered%22%3A%5B2%5D%2C%22Style%22%3A1%7D and https://artskart.artsdatabanken.no/app/#map/570099,8702127/6/background/greyMap/filter/%7B%22TaxonIds%22%3A%5B188851%2C188853%5D%2C%22AreaIds%22%3A%5B2449%5D%2C%22IncludeSubTaxonIds%22%3Atrue%2C%22Found%22%3A%5B2%5D%2C%22NotRecovered%22%3A%5B2%5D%2C%22Style%22%3A1%7D

Auwera, G. V. d., Carneiro, M. O., Hartl, C., Poplin, R., Del Angel, G., Levy-Moonshine, A., Jordan, T., Shakir, K., Roazen, D., Thibault, J., Banks, E., Garimella, K. V., Altshuler, D., Gabriel, S., & Depristo, M. A. (2013). From FastQ Data to High-Confidence Variant Calls: The Genome Analysis Toolkit Best Practices Pipeline. *Current Protocols in Bioinformatics, 43*(1).

Auwera, G. V. d., & O'Connor, B. D. (2020). *Genomics in the Cloud: Using Docker, GATK, and WDL in Terra*: O'Reilly Media.

Bailey, S. (2012). Principal Component Analysis with Noisy and/or Missing Data. *Publications of the Astronomical Society of the Pacific, 124*(919), 1015-1023.

Brown, C. M., Arbour, J. H., & Jackson, D. A. (2012). Testing of the Effect of Missing Data Estimation and Distribution in Morphometric Multivariate Data Analyses. *Systematic Biology, 61*(6), 941-954.

Burger, G., Gray, M. W., & Franz Lang, B. (2003). Mitochondrial genomes: anything goes. *Trends in Genetics, 19*(12), 709-716.

Catchen, J. M., Amores, A., Hohenlohe, P., Cresko, W., & Postlethwait, J. H. (2011). Stacks: Building and Genotyping Loci De Novo From Short-Read Sequences. *G3-Genes Genomes Genetics, 1*(3), 171-182.

Chong, J. P., Harris, J. L., & Roe, K. J. (2016). Incongruence between mtDNA and nuclear data in the freshwater mussel genus *Cyprogenia* (Bivalvia: Unionidae) and its impact on species delineation. *Ecology and Evolution, 6*(8), 2439-2452.

Coleman, C. O. (2015). Taxonomy in times of the taxonomic impediment – examples from the community of experts on amphipod crustaceans. *Journal of Crustacean Biology, 35*(6), 729-740.

Dewoody, J. A., Harder, A. M., Mathur, S., & Willoughby, J. R. (2021). The long-standing significance of genetic diversity in conservation. *Molecular Ecology, 30*(17), 4147-4154.

Duffy, A. M., Aguero, B., Stenøien, H. K., Flatberg, K. I., Ignatov, M. S., Hassel, K., & Shaw, A. J. (2020). Phylogenetic structure in the *Sphagnum recurvum* complex (Bryophyta) in relation to taxonomy and geography. *American Journal of Botany, 107*(9), 1283-1295.

Ehrich, D., Alsos, I. G., & Brochmann, C. (2008). Where did the northern peatland species survive the dry glacials: cloudberry (*Rubus chamaemorus*) as an example. *Journal of Biogeography, 35*(5), 801-814.

Elias, S. A., Short, S. K., & Birks, H. H. (1997). Late Wisconsin environments of the Bering Land Bridge. *Palaeogeography, Palaeoclimatology, Palaeoecology, 136*(1-4), 293-308.

Ewing, B., & Green, P. (1998). Base-Calling of Automated Sequencer Traces UsingPhred.II. Error Probabilities. *Genome Research, 8*(3), 186-194.

Flatberg, K. I. (1988). Taxonomy of *Sphagnum annulatum* and related species. *Annales Botanici Fennici, 25*(4), 303-350.

Flatberg, K. I. (1994). *Sphagnum tundrae*, a New Species in Sect. Squarrosa from the Arctic. *Lindbergia, 19*(1), 3-10.

Flatberg, K. I. (2007). Contributions to the *Sphagnum* Flora of West Greenland, with *Sphagnum concinnum* stat. et sp. nov. *Lindbergia, 32*(3), 88-98.

Flatberg, K. I. (2013). *Norges Torvmoser*. Trondheim: Akademika.

Gamfeldt, L., Hillebrand, H., & Jonsson, P. R. (2008). Multiple functions increase the importance of biodiversity for overall ecosystem functioning. *Ecology, 89*(5), 1223-1231.

GBIF_Secretariat. (2021). *Sphagnum squarrosum* Crome, 1803. *GBIF Backbone Taxonomy*.

Gutiérrez, E. E., & Garbino, G. S. T. (2018). Species delimitation based on diagnosis and monophyly, and its importance for advancing mammalian taxonomy. *Zoological Research, 39*(5), 301.

Hassel, K., Kyrkjeeide, M. O., Yousefi, N., Prestø, T., Stenøien, H. K., Shaw, A. J., & Flatberg, K. I. (2018). *Sphagnum divinum (sp. nov.)* and *S. medium* Limpr. and their relationship to *S. magellanicum* Brid. *Journal of Bryology, 40*(3).

Hedenäs, L. (2019). On the frequency of northern and mountain genetic variants of widespread species: essential biodiversity information in a warmer world. *Botanical Journal of the Linnean Society, XX*, 1-35.

Institute, N. P. (2019). toposvalbard.npolar.no. Retrieved from https://toposvalbard.npolar.no/

IPBES. (2019). Summary for policymakers of the global assessment report on biodiversity and ecosystem services of the Intergovernmental Science-Policy Platform on Biodiversity and Ecosystem Services. In S. Díaz, J. Settele, E. S. Brondízio, E.S., H. T. Ngo, M. Guèze, J. Agard, A. Arneth, P. Balvanera, K. A. Brauman, S. H. M. Butchart, K. M. A. Chan, L. A. Garibaldi, K. Ichii, J. Liu, S. M. Subramanian, G. F. Midgley, P. Miloslavich, Z. Molnár, D. Obura, A. Pfaff, S. Polasky, A. Purvis, J. Razzaque, B. Reyers, R. Roy Chowdhury, Y. J. Shin, I. J. Visseren-Hamakers, K. J. Willis, C. N. Zayas, & (eds.) (Eds.): IPBES secretariat, Bonn, Germany.

IPCC. (2021). Climate Change 2021: The Physical Science Basis. Contribution of Working Group I to the Sixth Assessment Report of the Intergovernmental Panel on Climate Change. In V. Masson-Delmotte, P. Zhai, A. Pirani, S. L. Connors, C. Péan, S. Berger, N. Caud, Y. Chen, L. Goldfarb, M. I. Gomis, M. Huang, K. Leitzell, E. Lonnoy, J. B. R. Matthews, T. K. Maycock, T. Waterfield, O. Yelekçi, R. Yu, B. Zhou, & (eds.) (Eds.). Cambridge University Press. In Press.

Izquierdo-Carrasco, F., Smith, S. A., & Stamatakis, A. (2011). Algorithms, data structures, and numerics for likelihood-based phylogenetic inference of huge trees. *BMC Bioinformatics, 12*(1), 470.

Jombart, T., & Ahmed, I. (2011). adegenet 1.3-1: new tools for the analysis of genome-wide SNP data. *Bioinformatics, 27*(21), 3070-3071.

Knaus, B. J., & Grünwald, N. J. (2017). vcfr: a package to manipulate and visualize variant call format data in R. *Molecular Ecology Resources, 17*(1), 44-53.

Kopelman, N. M., Mayzel, J., Jakobsson, M., Rosenberg, N. A., & Mayrose, I. (2015). Clumpak: a program for identifying clustering modes and packaging population structure inferences across K. *Molecular Ecology Resources, 15*, 1179–1191.

Korneliussen, T. S., Albrechtsen, A., & Nielsen, R. (2014). ANGSD: Analysis of Next Generation Sequencing Data. *BMC Bioinformatics*.

Kyrkjeeide, M. O., Hassel, K., Flatberg, K. I., Shaw, A. J., Brochmann, C., & Stenøien, H. K. (2016a). Long-distance dispersal and barriers shape genetic structure of peatmosses (*Sphagnum*) across the Northern Hemisphere. *Journal of Biogeography, 43*, 1215-1226.

Kyrkjeeide, M. O., Hassel, K., Flatberg, K. I., Shaw, A. J., Yousefi, N., & Stenøien, H. K. (2016b). Spatial Genetic Structure of the Abundant and Widespread Peatmoss Sphagnum magellanicum Brid. *PLoS ONE*. doi:DOI:10.1371/journal.pone.0148447

Kyrkjeeide, M. O., Hassel, K., Stenøien, H. K., Prestø, T., Boström, E., Shaw, A. J., & Flatberg, K. I. (2015). The dark morph of *Sphagnum fuscum* (Schimp.) H.Klinggr. in Europe is conspecific with the North American *S. beothuk*. *Journal of Bryology, 37*(4), 251-266.

Lewis, L. R., Behling, E., Gousse, H., Qian, E., Elphick, C. S., Lamarre, J.-F., Bêty, J., Liebezeit, J., Rozzi, R., & Goffinet, B. (2014). First evidence of bryophyte diaspores in the plumage of transequatorial migrant birds. *PeerJ, 2*, e424.

Li, H., & Durbin, R. (2009). Fast and accurate short read alignment with Burrows-Wheeler transform. *Bioinformatics, 25*(14), 1754-1760.

López-Rojo, N., Pérez, J. P. J., Basaguren, A., Martínez, A., Tonin, A. M., Correa-Araneda, F., & Boyero, L. (2019). Plant diversity loss affects stream ecosystem multifunctionality. *Ecology, 100*(12).

Meleshko, O., Martin, M. D., Korneliussen, T. S., Schröck, C., Lamkowski, P., Schmutz, J., Healey, A., Piatkowski, B. T., Shaw, A. J., Weston, D. J., Flatberg, K. I., Szövényi, P., Hassel, K., & Stenøien, H. K. (2021). Extensive Genome-Wide Phylogenetic Discordance Is Due to Incomplete Lineage Sorting and Not Ongoing Introgression in a Rapidly Radiated Bryophyte Genus. *Molecular Biology and Evolution, 38*(7), 2750-2766.

Meleshko, O., Stenøien, H. K., Speed, J. D. M., Flatberg, K. I., Kyrkjeeide, M. O., & Hassel, K. (2018). Is interspecific gene flow and speciation in peatmosses (*Sphagnum*) constrained by phylogenetic relationship and life-history traits? *Lindbergia, 41*(1).

Neilson, R. P., Pitelka, L. F., Solomon, A. M., Nathan, R., Midgley, G. F., Fragoso, J. M. V., Lischke, H., & Thompson, K. (2005). Forecasting Regional to Global Plant Migration in Response to Climate Change. *BioScience, 55*(9), 749.

Nordal, I. (1987). Tabula Rasa After All? Botanical Evidence for Ice-Free Refugia in Scandinavia Reviewed. *Journal of Biogeography, 14*(4), 377-388.

Padial, J. M., Castroviejo-Fisher, S., Köhler, J., Vilà, C., Chaparro, J. C., & De La Riva, I. (2009). Deciphering the products of evolution at the species level: the need for an integrative taxonomy. *Zoologica Scripta, 38*(4), 431-447.

Patiño, J., & Vanderpoorten, A. (2018). Bryophyte Biogeography. *Critical Reviews in Plant Sciences, 37*(2-3), 175-209.

Peterson, K. M. (2014). Plants in Arctic Environments. In Russell K. Monson (Ed.), *Ecology and the Environment* (1 ed.). New York: Springer.

Pritchard, J. K., Stephens, M., & Donnelly, P. (2000). Inference of Population Structure Using Multilocus Genotype Data. *Genetics, 155*(2), 945-959.

R-Core-Team. (2019). R: A language and environment for statistical computing. R Foundation for Statistical Computing, Vienna, Austria. Retrieved from http://www.r-project.org/index.html

Rambaut, A. (2018). FigTree (Version 1.4.4): University of Edinburgh. Retrieved from https://github.com/rambaut/figtree/releases

Renner, M. (2020). Opportunities and challenges presented by cryptic bryophyte species. *Telopea, 23*, 41-60.

Rieppel, O. (2010). Species monophyly. *Journal of Zoological Systematics and Evolutionary Research, 48*(1), 1-8.

Schwarzer, C., & Joshi, J. (2017). Parallel adaptive responses to abiotic but not biotic conditions after cryptic speciation in European peat moss *Sphagnum magellanicum* Brid. *Perspectives in Plant Ecology, Evolution and Systematics, 26*, 14-27.

Shaw, A. J., Flatberg, K. I., Szövényi, P., Ricca, M., Johnson, M. G., Stenøien, H. K., & Shaw, B. (2012). Systematics of the *Sphagnum fimbriatum* Complex: Phylogenetic Relationships, Morphological Variation, and Allopolyploidy. *Systematic botany, 37*(1), 15-30.

Shaw, A. J., & Goffinet, B. (2008). Bryophyte species and speciation. In Arthur Jonathan Shaw (Ed.), *Bryophyte Biology* (pp. 445-486): Cambridge University Press.

Society, B. B. (2010). *Sphagnum squarrosum*. In Ian Atherton, Sam Bosanquet, & Mark Lawley (Eds.), *Mosses and Liverworts of Britain and Ireland - a field guide* (pp. 281). United Kingdom: Latimer Trend & Co. Ltd, Plymouth.

Stamatakis, A. (2018). RAxML (Version 8.2.12): The Exelis Lab.

Stenøien, H. K., Hassel, K., Segreto, R., Gabriel, R., Karlin, E. F., Shaw, A. J., & Flatberg, K. I. (2014). High morphological diversity in remote island populations of the peat moss *Sphagnum palustre*: glacial refugium, adaptive radiation or just plasticity? *The Bryologist, 117*(2), 95-109.

Sundberg, S. (2013). Spore rain in relation to regional sources and beyond. *Ecography, 36*(3), 364-373.

Suzuki, H. (1967). Notes on the section Squarrosa of *Sphagnum* in Japan. *Journal of Science of the Hiroshima University, 11*.

Szövényi, P., Hock, Z., Schneller, J. J., & Tóth, Z. (2007). Multilocus dataset reveals demographic histories of two peat mosses in Europe. *Bmc Evolutionary Biology, 7*(1), 144.

Szövényi, P., Hock, Z., Urmi, E., & Schneller, J. J. (2006). Contrasting phylogeographic patterns in *Sphagnum fimbriatum* and *Sphagnum squarrosum* (Bryophyta, Sphagnopsida) in Europe. *New Phytologist, 172*, 784-794.

Szövényi, P., Sundberg, S., & Shaw, A. J. (2012). Long-distance dispersal and genetic structure of natural populations: an assessment of the inverse isolation hypothesis in peat mosses. *Molecular Ecology, 21*(22), 5461-5472.

Tropicos. (2021). *Sphagnum squarrosum*, Tropicos, botanical information system at the Missouri Botanical Garden Retrieved from https://tropicos.org/name/Search?name=sphagnum%20squarrosum

Tsutsui, K., Suwa, A., Sawada, K. I., Kato, T., Ohsawa, T. A., & Watano, Y. (2009). Incongruence among mitochondrial, chloroplast and nuclear gene trees in *Pinus* subgenus *Strobus* (Pinaceae). *Journal of Plant Research, 122*(5), 509-521.

Vanderpoorten, A., & Goffinet, B. (2009). Origin and evolution of bryophyte distribution patterns. In *Introduction to Bryophytes*. United Kingdom: Cambridge university press.

Vanderpoorten, A., Laenen, B., Gabriel, R., González-Mancebo, J. M., Rumsey, F. J., & Carine, M. A. (2011). Dispersal, diversity and evolution of the Macaronesian cryptogamic floras. In David Bramwell & Juli Caujapé-Castells (Eds.), *The Biology of Island Floras* (pp. 338-364). Cambridge: Cambridge University Press.

Vigalondo, B., Garilletib, R., Vanderpoorten, A., Patiñod, J., Drapera, I., J.A. Callejaf, Mazimpakaa, V., & Laraa, F. (2019). Do mosses really exhibit so large distribution ranges? Insights from the integrative taxonomic study of the *Lewinskya affinis* complex (Orthotrichaceae, Bryopsida). *Molecular phylogenetics and evolution, 140*.

Wang, J. (2017). The computer program structure for assigning individuals to populations: easy to use but easier to misuse. *Molecular Ecology Resources, 17*(5), 981-990.

Wang, Y., Lu, J., Yu, J., Gibbs, R. A., & Yu, F. (2013). An integrative variant analysis pipeline for accurate genotype/haplotype inference in population NGS data. *Genome Research, 23*(5), 833-842.

Westergaard, K. B., Zemp, N., Bruederle, L. P., Stenøien, H. K., Widmer, A., & Fior, S. (2019). Population genomic evidence for plant glacial survival in Scandinavia. *Molecular Ecology, 28*(4), 818-832.

Winston, J. E. (1999). *Describing species: practical taxonomic procedure for biologists*. New York, USA: Columbia University press.

Wright, B., Farquharson, K. A., McLennan, E. A., Belov, K., Hogg, C. J., & Grueber, C. E. (2019). From reference genomes to population genomics: comparing three reference-aligned reduced-representation sequencing pipelines in two wildlife species. *BMC Genomics, 20*(1).

Yousefi, N., Hassel, K., Flatberg, K. I., Kemppainen, P., Trucchi, E., Shaw, A. J., Kyrkjeeide, M. O., Szövényi, P., & Stenøyen, H. K. (2017). Divergent evolution and niche

differentiation within the common peatmoss *Sphagnum magellanicum*. *American Journal of Botany, 104*(7), 1060-1072.

Yousefi, N., Mikulášková, E., Stenøien, H. K., Flatberg, K. I., Košuthová, A., Hájek, M., & Hassel, K. (2019). Genetic and morphological variation in the circumpolar distribution range of *Sphagnum warnstorfii*: indications of vicariant divergence in a common peatmoss. *Botanical Journal of the Linnean Society, 189*(4), 408-423.

Yu, Z., Beilman, D. W., Frolking, S., Macdonald, G. M., Roulet, N. T., Camill, P., & Charman, D. J. (2011). Peatlands and Their Role in the Global Carbon Cycle. *Eos, Transactions American Geophysical Union, 92*(12), 97-98.

Yu, Z., Loisel, J., Brosseau, D. P., Beilman, D. W., & Hunt, S. J. (2010). Global peatland dynamics since the Last Glacial Maximum. *Geophysical research letters, 37*.

Appendix

Table 1: Utilization of study samples and presence of voucher material and material from the common garden experiment. For microsatellite and RAD-seq analysis columns, green cell with an X means utilized in said study, and red empty cell means not utilized in said study.

Species	Sample name	herbariumID	voucher	Common garden		microsatellite	RAD-seq analysis
			herbariumID	herbariumID	Nr. Of duplicates		
S. compactum	AI9	111910					x
S. lindbergii	NJ210	111989					x
S. squarrosum	AG7	112042					x
S. squarrosum	MS01	118979		118980	4	x	x
S. squarrosum	MS02	118975		118976	4	x	x
S. squarrosum	MS04	93529					x
S. squarrosum	MS05	120307					x
S. squarrosum	MS06	96444					x
S. squarrosum	MS07	96909					x
S. squarrosum	MS08	96484					x
S. squarrosum	MS09	96485					x
S. squarrosum	MS10	108921					x
S. squarrosum	MS12	120293					x
S. squarrosum	MS13	11879					x
S. squarrosum	MS15	693768					x
S. squarrosum	MS16	8969					x
S. squarrosum	NG7	112048					x
S. squarrosum	ST02	693764				x	x
S. squarrosum	T02	118903					x
S. squarrosum	T11	118911					x
S. squarrosum	T15	118928	118916			x	x
S. squarrosum	T16	118917	118916				x
S. squarrosum	T23	118929	118927	118926	3	x	
S. squarrosum	T26	118932	118933	118937	2	x	
S. squarrosum	T32	118939	118940	118941	4		x
S. squarrosum	T36	118944				x	
S. squarrosum	T37	118945	118946	118947	2	x	
S. squarrosum	T42	118954	118955			x	x
S. squarrosum	T46	118960	118961	118962	3	x	x
S. squarrosum	T48	118963		118964	4		x
S. squarrosum	T50	118965		118966	7		x
S. squarrosum	T53	118969	118970				x

Species	Sample name	herbariumID	voucher	Common garden		microsatellite	RAD-seq analysis
			herbariumID	herbariumID	Nr. Of duplicates		
S. teres	MT01	118977		118978	3	x	
S. teres	MT02	118973		118974	5	x	x
S. teres	MT03	93574					x
S. teres	MT06	96974					x
S. teres	MT07	96975					x
S. teres	MT08	108548					x
S. teres	MT09	108551					x
S. teres	MT10	96483					x
S. teres	MT11	96486					x
S. teres	MT12	93579					x
S. teres	MT13	93508					x
S. teres	MT14	11464					x
S. teres	ST01	741168				x	
S. teres	T07	118906					x
S. teres	T09_2	118908					x
S. teres	T13	118913					x
S. teres	T17	118918	118919				x
S. teres	T18	118920					x
S. teres	T20	118923					x
S. teres	T25	118930	118931			x	x
S. teres	T29	118935		118938	2		x
S. teres	T39	118948	118949	118950	3		x
S. teres	T52	118967	118968			x	x
S. tundrae	MU02	9626					x
S. tundrae	MU05	9632					x
S. tundrae	ST03	693791				x	
S. tundrae	T03	118902					x
S. tundrae	T04	118904					x
S. tundrae	T05	118971					x
S. tundrae	T14	118914					x
S. tundrae	T19	118921					x
S. tundrae	T34	118942		118943	3	x	x
S. tundrae	T41	118952	118953				x
S. tundrae	T43	118956	118957				x
S. tundrae	T45	118959				x	x

Table 2: Study sample information

Species	Sample name	herbariumID	Country	Date	Locality	County	Place	Habitat	Longitude	Latitude
S. compactum	AI9	111910	Norway	08/09/17	Draksten, mire N of Svarttjønnåsen	Trøndelag		Pure fen lawn	10.66901	63.31293
S. lindbergii	NJ210	111989	Norway	10/03/17	E of Langvatnet by Daltjønnbakken (Daltjønna)	Trøndelag		Intermediate fen carpet	11.45651	64.26684
S. squarrosum	AG7	112042	Norway	08/09/17	Draksten, mire N of Svarttjønnåsen	Trøndelag	Svarttjønnåsen	spring influenced sloping fen, spruce forest	11.45651	64.26684
S. squarrosum	MS01	118979	Norway	17/09/19	Postmyra	Trøndelag	Klæbu	Swampy spruce forest	10.4195	63.2769
S. squarrosum	MS02	118975	Norway	17/09/19	Motunmyra	Trøndelag	Klæbu	Swampy spruce forest	10.4424	63.2703
S. squarrosum	MS04	93529	Faroe	04/07/17	Streymoy, Sornfelli	Streymoy	Streymoy	Moist heath	-6.9633	62.0746
S. squarrosum	MS05	120307	Estonia	17/08/12	Niinsaare bog	Ida-Virumaa	Ida-Virumaa	Mire forest ditch	27.553	59.2541
S. squarrosum	MS06	96444	Norway	13/10/19	Postmyra	Trøndelag	Klæbu	Moist spruce forest, border to mire	10.419	63.2768
S. squarrosum	MS07	96909	Norway	13/10/19	Postmyra.	Trøndelag	Klæbu	Swampy spruce forest.	10.419	63.2768
S. squarrosum	MS08	96484	Finland	05/08/19	Viiankiaapa mire	Lapland	Sodankylä	Intermediate rich fen	26.7685	67.5729
S. squarrosum	MS09	96485	Finland	05/08/19	Viiankiaapa mire	Lapland	Sodankylä	Intermediate rich fen beside a birch	26.7685	67.5729
S. squarrosum	MS10	108921	Norway	21/07/19	Seglvikelva, ved stien til Finnkirka.	Finnmark	Lebesby	Sump med vierkratt og spredte lauvtrær.	27.275	70.9499
S. squarrosum	MS12	120293	Estonia	16/08/12	Äntu lakes	Ida-Virumaa	Lääne-Virumaa	Rich mire forest	26.239	59.049
S. squarrosum	MS13	11879	Iceland	02/08/12	Austurland	Austurland	Iceland	Tjarnastararflóavist	-14.2596	65.4542
S. squarrosum	MS15	693768	Greenland	16/08/10	Nuuk, Kobbefjord, Nukk basic study area	Sermersooq		Poor fen	-51.3884	64.1308
S. squarrosum	MS16	8969	Greenland	26/07/13	Queqertarsuaq, Disko.	Qaasuitsup		Sedge-dominated, moist slope.	-53.4927	69.2576
S. squarrosum	NG7	112048	Norway	10/03/17	Namsos	Trøndelag		swampy birch forest	11.45651	64.26684
S. squarrosum	ST02	693764	Norway	16/08/11	Nuuk, Kobbefjord, Nuuk basic study area	Sermersooq	Greenland	Poor fen by river	-51.3815	64.1335
S. squarrosum	T02	118903	Svalbard	20/08/19	Bjørndalen	Nordenskiöld land	Spitsbergen, Svalbard		15.3113	78.2054
S. squarrosum	T11	118911	Svalbard	20/08/19	Bjørndalen	Nordenskiöld land	Spitsbergen, Svalbard		15.3356	78.2094
S. squarrosum	T15	118928	Svalbard	21/08/19	Bolterdalen	Nordenskiöld land	Spitsbergen, Svalbard	Arctic tundra, moist slope	15.989	78.1521
S. squarrosum	T16	118917	Svalbard	21/08/19	Bolterdalen	Nordenskiöld land	Spitsbergen, Svalbard	Arctic tundra, moist slope	15.989	78.1521
S. squarrosum	T23	118929	Svalbard	22/08/19	Blomsterdalen	Nordenskiöld land	Spitsbergen, Svalbard	Moist Cassiope heath	15.5139	78.2368
S. squarrosum	T26	118932	Svalbard	22/08/19	Blomsterdalen	Nordenskiöld land	Spitsbergen, Svalbard	Equisetum tundra, moist and sloping	15.517	78.2349
S. squarrosum	T32	118939	Svalbard	22/08/19	Endalen	Nordenskiöld land	Spitsbergen, Svalbard		15.7617	78.1841
S. squarrosum	T36	118944	Svalbard	22/08/19	Endalen	Nordenskiöld land	Spitsbergen, Svalbard	Alongside a stream, Arctic tundra, moist slope	15.7594	78.1837
S. squarrosum	T37	118945	Svalbard	22/08/19	Endalen	Nordenskiöld land	Spitsbergen, Svalbard	Arctic tundra, moist slope	15.7526	78.1824
S. squarrosum	T42	118954	Svalbard	23/08/19	Colesbukta	Nordenskiöld land	Spitsbergen, Svalbard	Arctic tundra, moist slope	15.0195	78.1193
S. squarrosum	T46	118960	Svalbard	23/08/19	Colesbukta	Nordenskiöld land	Spitsbergen, Svalbard	Slightly moist Arctic tundra, steep slope	15.0245	78.122
S. squarrosum	T48	118963	Svalbard	23/08/19	Colesbukta	Nordenskiöld land	Spitsbergen, Svalbard	Slight slope, moist Arctic tundra	15.0174	78.1227
S. squarrosum	T50	118965	Svalbard	23/08/19	Colesbukta	Nordenskiöld land	Spitsbergen, Svalbard	Slight slope, moist Arctic tundra	15.0201	78.1215
S. squarrosum	T53	118969	Svalbard	23/08/19	Longyeardalen	Nordenskiöld land	Spitsbergen, Svalbard	Arctic tundra, moist slope	15.5926	78.1998

Species	Sample name	herbariumID	Country	Date	Locality	County	Place	Habitat	Longitude	Latitude
S. teres	MT01	118977	Norway	17/09/19	Postmyra	Trøndelag	Norway, Trønderlag, Klæbu	rich fen	10.4195	63.2769
S. teres	MT02	118973	Norway	17/09/19	Momyra	Trøndelag	Norway, Trønderlag, Klæbu		10.4427	63.2704
S. teres	MT03	93574	Faroe	18/04/18	Streymoy, Tórshavnar	Streymoy	Streymoy	Moist, intermediate heath	-6.8061	62.0107
S. teres	MT06	96974	Norway	14/01/20	Bromsvika, N of Drageid.	Trøndelag	Trøndelag	Depression in coastal heath with Betula around.	10.6104	64.3895
S. teres	MT07	96975	Norway	14/01/20	Bromsvika, N of Drageid.	Trøndelag	Trøndelag	Depression in coastal heath with Betula around.	10.6104	64.3895
S. teres	MT08	108548	Norway	30/01/20	Søre Smådalen towards Ranastongnøse.	Møre og Romsdal	Innlandet, Møre og Romsdal	Edge of small pond.	8.5776	61.0292
S. teres	MT09	108551	Norway	30/01/20	Søre Smådalen towards Ranastongnøse.	Møre og Romsdal	Innlandet, Møre og Romsdal	Transition pond - heath.	8.5776	61.0292
S. teres	MT10	96483	Finland	09/12/19	Viiankiaapa mire	Lapland	Sompion Lappi	Mire margin, poor fen lawn	26.7648	67.574
S. teres	MT11	96486	Finland	09/12/19	Viiankiaapa mire	Lapland	Sompion Lappi	Intermediate rich fen	26.7685	67.5729
S. teres	MT12	93579	Faroe	18/04/18	Vágar, Leitisvatn, E side	Oeioe Islands	Vágar	Road side	-6.806	62.0107
S. teres	MT13	93508	Norway	17/04/18	Hovden	Trøndelag	Trøndelag	Northern boreal zone. Rich fen lawn	9.5086	62.6423
S. teres	MT14	11464	Norway	11/12/15	Trollsteinkvelven	Møre og Romsdal	Innlandet	Rich fen	8.5845	61.6841
S. teres	ST01	741168	Norway	21/06/11	Bunesfjorden, Moskenes	Nordland	Norway, Nordland	Rich fen lawn in road ditch	12.9923	67.9642
S. teres	T07	118906	Svalbard	20/08/19	Bjørndalen	Nordenskiöld land	Spitsbergen, Svalbard		15.3356	78.2094
S. teres	T09_2	118908	Svalbard	20/08/19	Bjørndalen	Nordenskiöld land	Spitsbergen, Svalbard		15.3356	78.2094
S. teres	T13	118913	Svalbard	20/08/19	Bjørndalen	Nordenskiöld land	Spitsbergen, Svalbard		15.3356	78.2094
S. teres	T17	118918	Svalbard	21/08/19	Bolterdalen	Nordenskiöld land	Spitsbergen, Svalbard	Arctic tundra, moist slope	15.9835	78.1511
S. teres	T18	118920	Svalbard	21/08/19	Bolterdalen	Nordenskiöld land	Spitsbergen, Svalbard	Arctic tundra, moist slope	15.9868	78.1445
S. teres	T20	118923	Svalbard	21/08/19	Bolterdalen	Nordenskiöld land	Spitsbergen, Svalbard	Cassiope tetragona + Arctic tundra, moist slope	15.988	78.1499
S. teres	T25	118930	Svalbard	22/08/19	Blomsterdalen	Nordenskiöld land	Spitsbergen, Svalbard	Sloping moist Cassiope heath	15.5164	78.235
S. teres	T29	118935	Svalbard	22/08/19	Blomsterdalen	Nordenskiöld land	Spitsbergen, Svalbard	Arctic tundra, moist slope	15.5153	78.2348
S. teres	T39	118948	Svalbard	22/08/19	Endalen	Nordenskiöld land	Spitsbergen, Svalbard	Wet slope, arctic tundra	15.7408	78.1844
S. teres	T52	118967	Svalbard	23/08/19	Colesbukta	Nordenskiöld land	Spitsbergen, Svalbard	Slight slope, moist Arctic tundra	15.0411	78.1139
S. tundrae	MU02	9626	Russia	21/08/14	Zabaikalsky Territory. Stanovoe Uplands. Kalar Dist. Kodar Range. Valley of Syni River.	Zabaykalsky Krai	Southern Siberia	Bush-Carex sp.-moss floodpain community. On turfs	117.37	56.1764
S. tundrae	MU05	9632	Russia	03/07/13	Zabaikalsky Territory. Kalar District, Kodar Range, valley of Srednii Sakukan River.	Zabaykalsky Krai	Southern Siberia	Moss community along stream.	117.8531	56.9169
S. tundrae	ST03	693791	Greenland	15/08/10	Nuuk, E of the church yard N of Grønlands Naturinstitutt	Sermersooq	Greenland	Intermediate mire	-51.6919	64.1942
S. tundrae	T03	118902	Svalbard	20/08/19	Bjørndalen	Nordenskiöld land	Spitsbergen, Svalbard		15.3113	78.2054
S. tundrae	T04	118904	Svalbard	20/08/19	Bjørndalen	Nordenskiöld land	Spitsbergen, Svalbard		15.3136	78.2021
S. tundrae	T05	118971	Svalbard	20/08/19	Bjørndalen	Nordenskiöld land	Spitsbergen, Svalbard		15.3136	78.2021
S. tundrae	T14	118914	Svalbard	21/08/19	Bolterdalen	Nordenskiöld land	Spitsbergen, Svalbard	Arctic tundra, moist slope	15.989	78.1521
S. tundrae	T19	118921	Svalbard	21/08/19	Bolterdalen	Nordenskiöld land	Spitsbergen, Svalbard	Arctic tundra, moist slope	15.9859	78.1457
S. tundrae	T34	118942	Svalbard	22/08/19	Endalen	Nordenskiöld land	Spitsbergen, Svalbard	Arctic tundra, moist slope	15.7617	78.1841
S. tundrae	T41	118952	Svalbard	22/08/19	Endalen	Nordenskiöld land	Spitsbergen, Svalbard	Moist Cassiope heath	15.7416	78.1846
S. tundrae	T43	118956	Svalbard	23/08/19	Colesbukta	Nordenskiöld land	Spitsbergen, Svalbard	Arctic tundra, moist slope	15.0221	78.1208
S. tundrae	T45	118959	Svalbard	23/08/19	Colesbukta	Nordenskiöld land	Spitsbergen, Svalbard	Slightly moist Arctic tundra, steep slope	15.024	78.1213

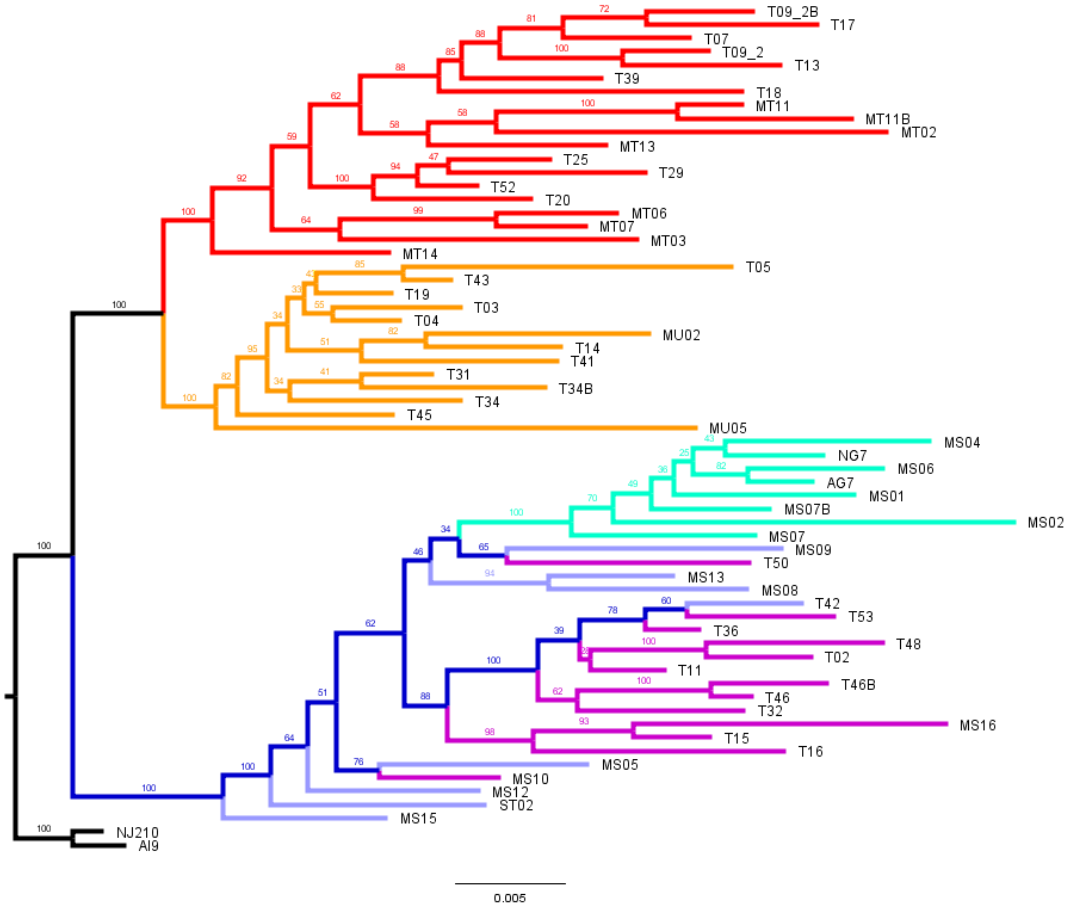

Figure 1: Phylogenetic tree using mitochondrial DNA, inferred with RAxML. Branch labels represent bootstrap values. S. teres is coloured red, S. tundrae is coloured yellow, and the branch holding S. squarrosum is coloured blue. Colours on the S. squarrosum branch are according to group colours seen in figure 11.

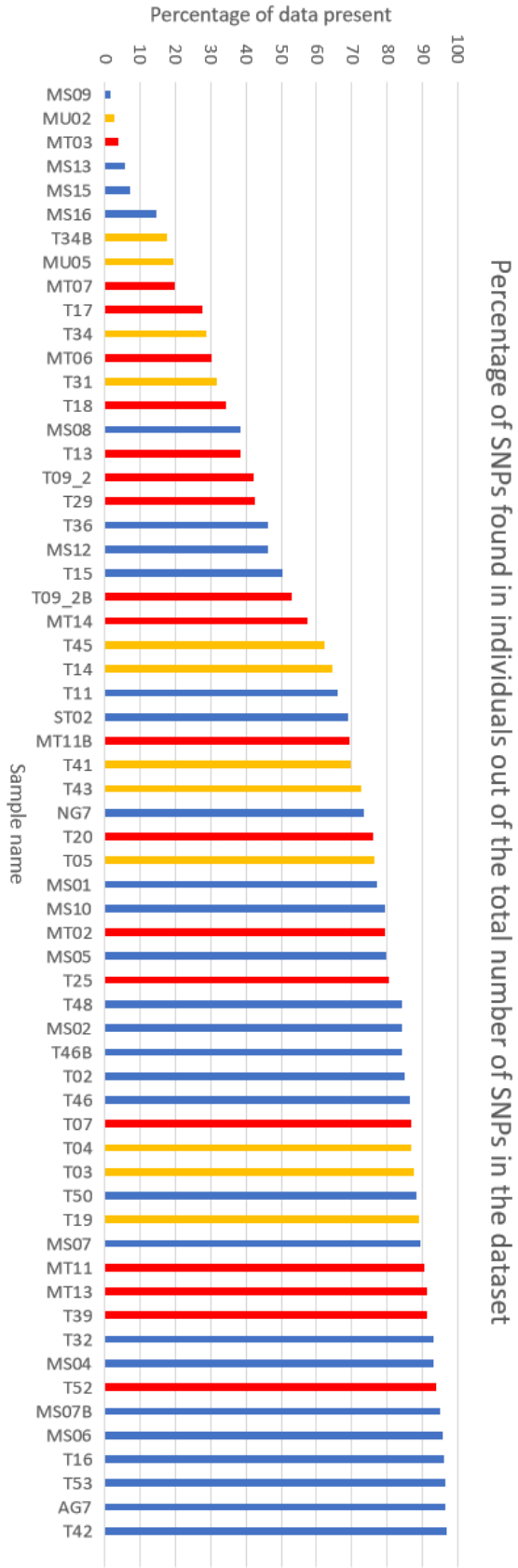

Figure 2:Missing data per sample, S. squarrosum is coloured blue, S. teres is red, and S. tundrae is orange.

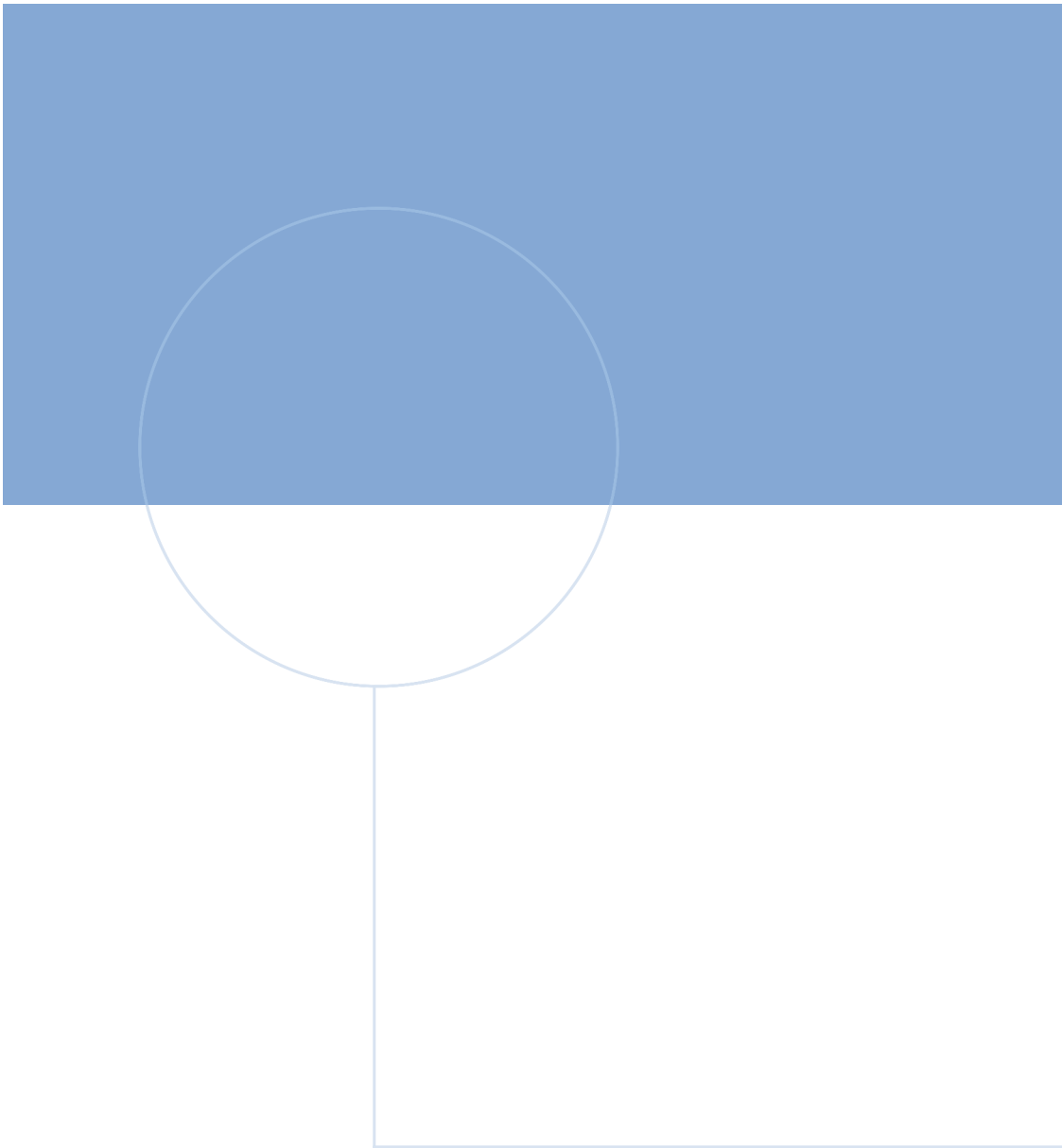

NTNU

Norwegian University of
Science and Technology